Food Sci. Biotechnol. Vol. 16, No. 5, pp. 691 ~ 709 (2007)

RESEARCH REVIEW

Food Science and Biotechnology

Potential Use of Biopolymer-based Nanocomposite Films in Food Packaging Applications

Jong-Whan Rhim

Department of Food Engineering, Mokpo National University, Muan, Jeonnam 534-729, Korea

Abstract Concerns on environmental waste problems caused by non-biodegradable petrochemical-based plastic packaging materials as well as consumer's demand for high quality food products has caused an increasing interest in developing biodegradable packaging materials using annually renewable natural biopolymers such as polysaccharides and proteins. However, inherent shortcomings of natural polymer-based packaging materials such as low mechanical properties and low water resistance are causing a major limitation for their industrial use. By the way, recent advent of nanocomposite technology rekindled interests on the use of natural biopolymers in the food packaging application. Polymer nanocomposites, especially natural biopolymer-layered silicate nanocomposites, exhibit markedly improved packaging properties due to their nanometer size dispersion. These improvements include increased mechanical strength, decreased gas permeability, and increased water resistance. Additionally, biologically active ingredients can be added to impart the desired functional properties to the resulting packaging materials. Consequently, natural biopolymer-based nanocomposite packaging materials with bio-functional properties have huge potential for application in the active food packaging industry. In this review, recent advances in the preparation and characterization of natural biopolymer-based nanocomposite films, and their potential use in food packaging applications are addressed.

Keywords: biodegradable, natural biopolymer, nanocomposite film, bionanocomposite, food packaging, antimicrobial packaging

Introduction

Packaging materials provide physical protection and create proper physicochemical conditions for products that are essential for obtaining a satisfactory shelf life. The packaging system, based on a proper choice of the packaging materials endowed with appropriate gas and water vapor barrier and mechanical properties, prevents product deterioration due to physicochemical or biological factors and maintains the overall quality during storage and handling. After their useful life, it is desirable for the packaging materials to biodegrade in a reasonable time period without causing environmental waste problems. In this sense, biopolymer-based packaging materials have some beneficial properties as packaging materials in improving food quality and extending the shelf-life through minimizing microbial growth in the product (1-5). Biopolymer films may also serve as gas and solute barriers and complement other types of packaging by improving the quality and extending the shelf-life of foods (6). Furthermore, biopolymer films are excellent vehicles for incorporating a wide variety of additives, such as antioxidants, antifungal agents, antimicrobials, colors, and other nutrients (6-8).

Natural biopolymers have the advantage over synthetic polymers in that they are biodegradable and renewable as well as edible. However, relatively poor mechanical and water vapor barrier properties of those films are causing a major limitation for their industrial use. Protein and polysaccharide films are generally good barriers against oxygen at low to intermediate relative humidity and have good mechanical properties; however, their barrier against water vapor is poor due to their hydrophilic nature (9, 10). Many research efforts have focused on improving the film properties of biopolymer-based films by the modification of biopolymer-based films to improve their mechanical and water vapor barrier properties (11-20). Though such efforts indicated a significant improvement in film properties, their physical, thermal, and mechanical properties are still not satisfactory and find difficulties in many applications.

On the other hand, polymer nanocomposite materials, having constituents with dimensions on the nanometer scale (10^{-9} m), are currently topics of intense research in the areas of polymer and material science, electronics, and biomedical science (21-23). A polymer nanocomposite is the hybrid material consisting of a polymer matrix reinforced with a fiber, platelet, or particle having one dimension on the nanometer scale (24). Owing to the nanometer-size particles dispersed in the polymer matrix, these nanocomposites exhibit markedly improved mechanical, thermal, optical, and physicochemical properties when compared with the pure polymer or conventional (microscopic) composites. Improvements can include, for example, increased moduli, strength and heat resistance, decreased gas permeability and flammability with very low filler loading, typically 5 wt% or lower (25).

Accordingly, biopolymers have been filled with layered silicates in order to enhance their desirable properties while maintaining their biodegradability. The impressive enhancements of the material properties of the nanocomposite films compared to the pure polymers can be achieved without the need for additional and cost-increasing processing or post-treatment procedures. Moreover, biodegradability is still retained, i.e., after final degradation,

*Corresponding author: Tel: 82-61-450-2423; Fax: 82-61-454-1521
E-mail: jwrhim@mokpo.ac.kr
Received January 12, 2007; accepted April 23, 2007

only inorganic, natural minerals (clay) will be left over (21, 26, 27).

Recent advances in the preparation, characterization, properties of biopolymer-based nanocomposite films, and their potential application in food packaging will be addressed in this review.

What is Nanocomposite Film?

Traditionally, mineral fillers such as clay, silica, and talc, are incorporated in film preparation in the range of 10 to 50 % by weight to reduce its cost or to improve its performance in some way. However, mechanical strength of the films, in general, decreases when fillers are present (28).

Recently, polymer-clay nanocomposites have received significant attention as an alternative to conventional filled polymers. Because of their nanometer-size dispersion, the polymer-clay nanocomposites exhibit the large-scale improvement in the mechanical and physical properties compared with pure polymer or conventional composites. These include increased modulus and strength, decreased gas permeability, increased solvent and heat resistance and decreased flammability (29). Since Toyota researchers in the late 1980's demonstrated that mechanical and flame retardant properties of nylon-clay composite material increased dramatically by reinforcing with less than 5% of clay (30), extensive research works have been performed in this area and several extensive review articles regarding recent advances in the production of nanocomposites with various polymers, their performance and application are available (21, 24, 25, 29, 31-37). Especially, Sinha Ray and Bousmina (31) and Pandey *et al.* (24) have comprehensively reviewed focusing on bidegradable nanocomposite materials.

Polymer-clay nanocomposites are a class of hybrid materials composed of organic polymer materials and nano-scale clay fillers (23, 38). Montmorillonite (MMT), hectorite, and saponite are frequently used pristine layered silicates, which are combined with polymeric materials to form nanocomposites (21). Among the nano-scale clays, MMT is of particular interest and has been studied widely. MMT is a clay mineral consisting of stacked silicate sheets with a high aspect ratio (ratio of length to thickness) and a plate-like morphology. This high aspect ratio (100-1,500) with high surface area (700-800 m^2/g) and platelet thickness of 1 nm plays an important role for the enhancement of mechanical and physical properties of composite materials (39). Chemically, MMT consists of 2 fused silicate tetrahedral sheets sandwiching an edge-shared octahedral sheet of either magnesium or aluminum hydroxide (21, 23, 25) as shown schematically in Fig. 1. Stacking of these layers form a van der Waals gap between the layers, which is called the 'interlayer' or the 'gallery'.

These clays usually contain hydrated sodium or potassium ions (29) and in this state these silicates are miscible only with hydrophilic polymers such as poly (ethylene oxide) (PEO), poly(vinyl alcohol) (PVOH), and natural biopolymers such as starches and proteins (21, 24). However, the hydrophilic nature of the MMT surface impedes its homogeneous dispersion in an organic polymer phase (21, 25). Therefore, it is very crucial to induce the organophilicity of MMT to be compatible with the organic polymer.

In the interlayer region of MMT there exists Na^+ and Ca^{2+}, which can be replaced by the alkylammonium and alkylphosphonium ions, rendering the clay into organophilic nature. Such modified clays are commonly referred to as organoclays. The organoclays play an important role for producing the nanocomposite. Surface modification may either enhance the interaction between the clay and the polymer, making it more suitably mixed, or it may favor the intercalation of the polymer chain by dictating the gallery spacing (40, 41). Schematic representation of surface modification of MMT is shown in Fig. 2. Surface modification of MMT causes to swell the interlayer space up to a certain extent (normally over 2 nm) and hence reduces the attraction between layers, which allows a favorable diffusion and accommodation of polymer into the interlayer space.

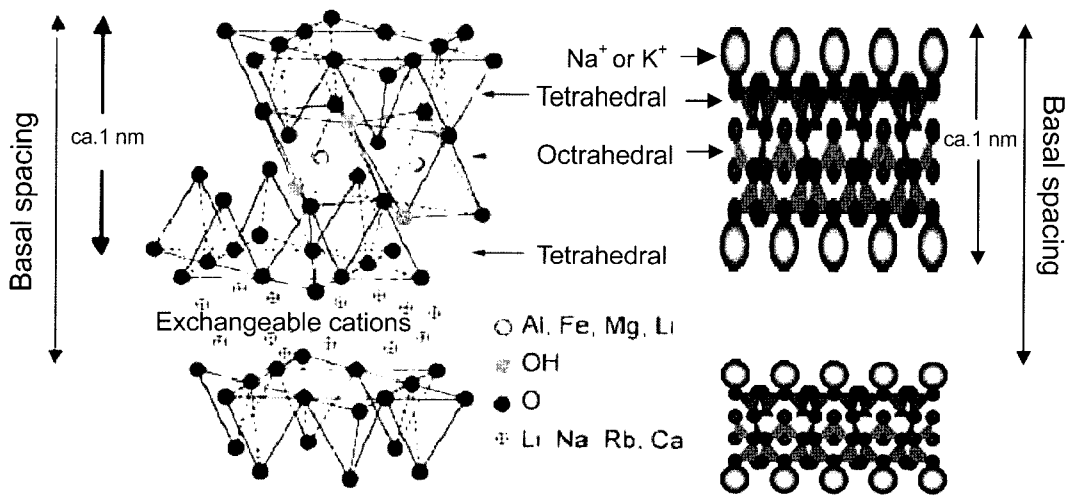

Fig. 1. Structure of 2:1 phyllosilicates. (ref. 31; http://www.wwnorton.com/college/chemistry/chemconnections/Rain/moviepages/montmorillonite_layers.htm)

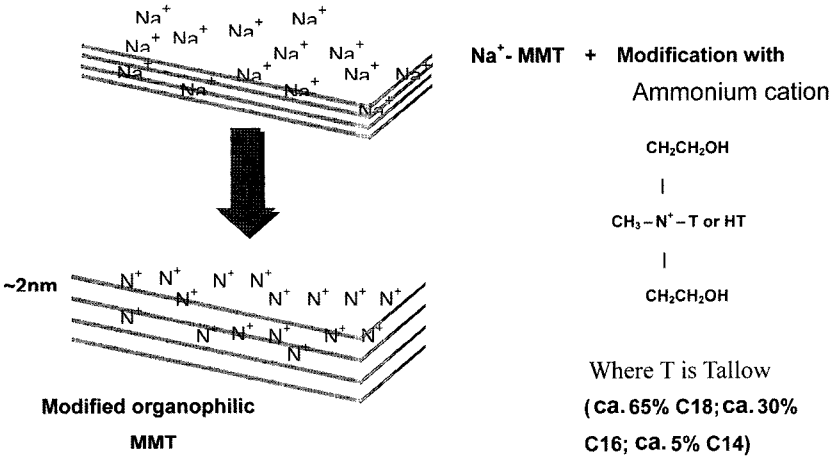

Fig. 2. Schematic representation of organic modification of layered silicate. (http://www.nanocor.com; http://www.nanoclay.com/data/30B.htm)

Preparation and Characterization

Preparation of nanocomposites Various methods have been used to synthesize polymer-clay nanocomposites, and their properties have been found to be dependent on the preparation procedure (42-45). *In situ* polymerization, solvent intercalation/exfoliation and melt intercalation/exfoliation are the 3 major methods for the formation of nanocomposites. *In situ* polymerization involves the combination of clay and monomer, followed by the polymerization of the monomer, which ideally locks the exfoliated clay particles in the resulting polymer matrix. In solution intercalation, the clay is first swollen in a solvent and the polymer (intercalant) is dissolved in the solvent. Both solutions are then combined, and the polymer chains intercalate and displace the solvent within the interlayer of the clay (42). In melt intercalation, the clay and polymer are added together above the melting temperature of the polymer; they may be held at this temperature for a period of time, put under shear, or other conditions to encourage intercalation and exfoliation of the clay. Of these, melt intercalation is the most appealing approach because of its versatility, its compatibility with current polymer processing equipment such as extrusion and injection molding, and its environmentally benign character due to the absence of solvents (42). In addition, the melt intercalation method allows the use of polymers which were previously not suitable for *in situ* polymerization or solution intercalation.

The solution intercalation method is good for the intercalation of polymers with little or no polarity into layered structure, and facilitates production of thin films with polymer-oriented clay intercalated layers. This technique has been widely used with water-soluble polymers to produce intercalated nanocomposites such as PEO (46-48) and PVOH (47, 49, 50). This method has been also applied for the preparation of nanocomposites with non-aqueous solvent-soluble polymers including polycaprolactone (PCL)/clay (51) and polylactide (PLA)/clay (52) in chloroform as a co-solvent, and high-density polyethylene (HDPE) with xylene and benzonitrile (53). Basically, the solvent intercalation technique is similar to the solvent casting method for the preparation of biopolymer films (2-5). Therefore, this technique can be easily adopted for the preparation of nanocomposite films with various natural biopolymers.

Characterization of nanocomposites When the layered silicate clays are mixed with a polymer, 3 types of composites are commonly obtained: i) immiscible tactoid, ii) intercalated, and iii) exfoliated structures (Fig. 3). In immiscible tactoids, complete clay particles are dispersed within the clay matrix and the layers do not separate. The mixture of polymer and the silicate clays are microscale composites, and the clay only serves as conventional filler. Intercalation and exfoliation produce 2 ideal nanoscale composites. In an intercalated nanocomposite often a single polymer chain will be driven between the clay silicate layers, but the system still remains quite well ordered in a stacked type of arrangement. In an exfoliated nanocomposite the silicate layers are completely delaminated from each other and are well dispersed. It is this second type - the exfoliated nanocomposite, which has been shown

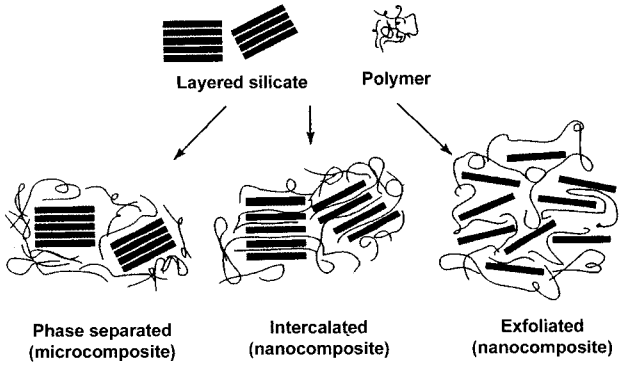

Fig. 3. Types of composite structure of polymer-layered silicate clay materials. (ref. 85)

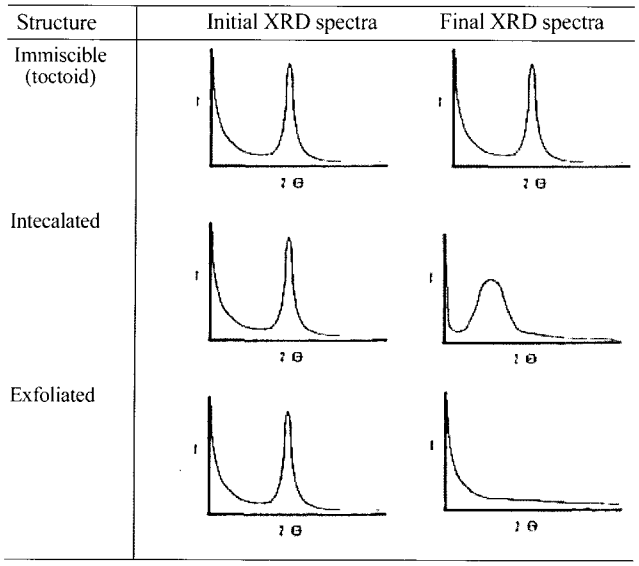

Fig. 4. Schematic representation of the X-ray diffraction patterns for various types of nanocomposite structures. (ref. 22)

to exhibit the most significant improvements in physical properties (54). The formation of intercalation or exfoliation depends on the type of clays and upon the processing conditions (55).

The structure of polymer nanocomposites is generally characterized by X-ray diffraction (XRD) and transmission electron microscopy (TEM). The composite structures such as tactoid, intercalated, or exfoliated structures of polymer/clay hybrid can be determined using XRD measurements by monitoring the position, shape, and intensity of the basal reflections of XRD patterns of the materials as shown schematically in Fig. 4. For immiscible polymer/clay hybrids, the structure of the silicate is not affected, and thus, the characteristics of the clay basal reflection do not change. On the other hand, the finite layer expansion associated with intercalated structures results in a new basal reflection that corresponds to the large gallery height of the intercalated hybrid. In contrast, the extensive layer separation associated with exfoliated structures disrupts the coherent layer stacking and results in no coherent X-ray diffraction pattern. Generally, the intercalated layered silicate has a defined interlayer spacing basal reflection corresponding to the d_{001} spacing in a XRD diffractogram. The basal (d_{001}) spacing between the layers of intercalated nanocomposite structures can be determined by the diffraction peak in the XRD patterns using the Bragg diffraction equation:

$$2\, d_{001}\sin\theta = \lambda$$

where d_{001} is the interplanar distance of (001) diffraction face, θ is the diffraction position, and λ is the wavelength. Although XRD offers a convenient method to determine the interlayer spacing of the silicate layers in the intercalated nanocomposites (within 1-4 nm), little can be said about the spatial distribution of the silicate layers or any structural non-homogeneities in nanocomposites (31). Therefore, conclusions concerning the mechanism of nanocomposites formation and their structure based solely on XRD patterns are only tentative. As a complementary technique to XRD, TEM allows a qualitative understanding of the internal structure, spatial distribution and dispersion of the silicate layers within the polymer matrix, and views of the nanocomposite structure through direct visualization (21, 36).

Table 1. Properties of nylon-6 and nylon-6/clay nanocomposite[1)]

Property	Nylon-6	Nylon-6/clay nanocomposite
Tensile modulus (GPa)	1.1	2.1
Tensile strength (MPa)	69	107
Heat distortion temp. (°C)	65	145
Impact strength (kJ/m^2)	2.3	2.8
Water adsorption (%)	0.87	0.51
Coeff. of thermal expansion	13×10^{-5}	6.3×10^{-5}

[1)]Ref. 29.

Properties of Nanocomposites

Mechanical properties Formation of nanocomposite with organoclays has shown pronounced improvement in the mechanical properties of various polymers substantially even with a low level of filler loading. Such advantage of nanocomposite was first demonstrated by a group at the Toyota Research Center in Japan with nylon/silicate nanocomposite (29, 54). Properties of nylon and nylon/clay nanocomposites containing 4% silicate are summarized in Table 1. This result shows profound enhancement in mechanical properties e.g., an increase in tensile modulus of 91%, and in tensile strength of 55%. Note the significant reduction in water adsorption for the nanocomposite. It has been frequently observed that mechanical properties of polymer/clay nanocomposites are strongly dependent on filler content. Huang and Yu (56) determined tensile properties of starch/MMT nanocomposites prepared with various filler concentrations of 0 to 11 wt% to the starch. Tensile test results are presented in Fig. 5. Tensile strength increased monotonously with increase in filler content up to 8%, then leveled off. Tensile strain decreased with

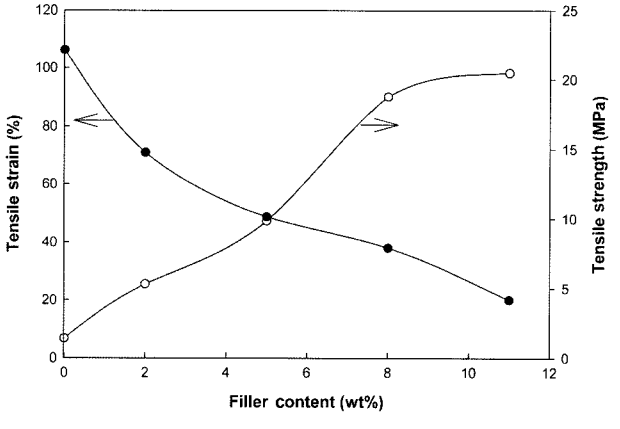

Fig. 5. Effect of filler content on tensile strength and tensile strain of starch/montmorillonite nanocomposites. (ref. 56)

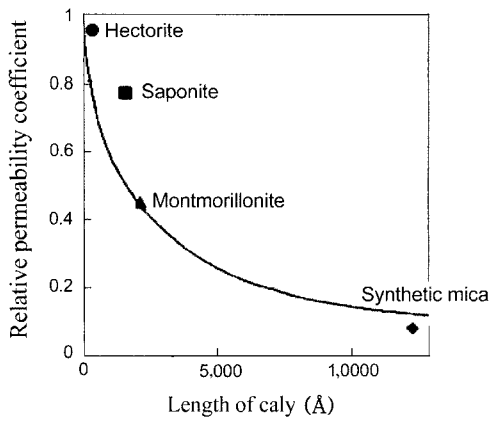

Fig. 6. Effect of clay length on relative permeability coefficient of nanocomposite films. (ref. 57)

increase in filler loading since clay usually leads to a brittle matrix. In their study, the optimum filler content was determined to be 8% based on the tensile properties. It is noteworthy that exfoliation of starch with 8% of clay loading increased tensile strength and tensile strain by 270 and 25%, respectively. Interestingly, the substantial increase in strength is not accompanied by a decrease in strain as is usually the case with filled polymers.

The enhancement in mechanical properties of polymer nanocomposites can be attributed to the high rigidity and aspect ratio together with the good affinity between polymer and organoclay.

Barrier properties Polymer nanocomposites have excellent barrier properties against gases (e.g., oxygen and carbon dioxide) and water vapor. Studies have shown that such reduction in permeability strongly depends on the aspect ratio of clay platelets, with high ratios dramatically enhancing gaseous barrier properties. Yano *et al.* (57) prepared polyimide/clay nanocomposite films with 4 different sizes of clay minerals such as hectorite, saponite, MMT, and synthetic mica in order to investigate the effect of the aspect ratio on the barrier properties of the hybrids. They found that, at constant clay content (2 wt%), the relative permeability coefficient decreased exponentially on increasing the length of the clay (Fig. 6). Yano *et al.* (58) also showed that gas permeability including water vapor permeability and oxygen gas permeability of polyimids/clay nanocomopsite films decrease exponentially with increase in clay content from 0 to 8 wt%. Generally the best gas barrier properties would be obtained in polymer nanocomposites with fully exfoliated clay minerals with large aspect ratio.

The increase in gas barrier properties of nanocomposite films is believed to be due to the presence of ordered dispersed silicate layers with large aspect ratios in the polymer matrix which are impermeable to water molecules (57, 59). This forces gas traveling through the film to follow a tortuous path through the polymer matrix surrounding the silicate particles (Fig. 7), thereby increasing the effective path length for diffusion.

The enhanced gas barrier properties of nanocomposites make them attractive and useful in food packaging applications, both flexible and rigid. Specific examples include packaging for processed meats, cheese, confectionery, cereals, and boil-in-bag foods, also extrusion-coating applications in association with paperboard for fruit juice and dairy products, together with co-extrusion processes for the manufacture of beer and carbonated drinks bottles. The use of nanocomposite formulations is expected to considerably enhance the shelf-life of many types of food. It provides gas barriers to carbon dioxide and oxygen resulting in a shelf-life up to 3-6 months for beers and fruit juices and up to one year for carbonated soft drink (60).

Degradation properties Another interesting property is the significantly improved biodegradability of nanocomposites made from organoclay and biodegradable polymers. Study on the biodegradability of nanocomposites based on poly(ε-caprolactone) (PCL) showed on improved biodegradability over pure PCL (61). Such an improved biodegradability of PCL in clay-based nanocomposites may be attributed to catalytic role of the organoclay in the biodegradation mechanism. Sinha Ray *et al.* (62-64) reported that the biodegradability of PLA nanocomposite made from organoclay is significantly enhanced. They attributed such a behavior to the presence of terminal hydroxylated edge groups in the clay layers. An interesting result regarding the biodegradability of aliphatic polyester (APES)/organoclay (Cloisite 30B) nanocomposites has been reported by Lee *et al.* (65). As shown in Fig. 8, they found rate of biodegradability of the nanocomposite decreased compared to the pristine polymer (APES), and the more loading of nanoclay incorporated, the lower the biodegradability of the naocomposite was observed. They

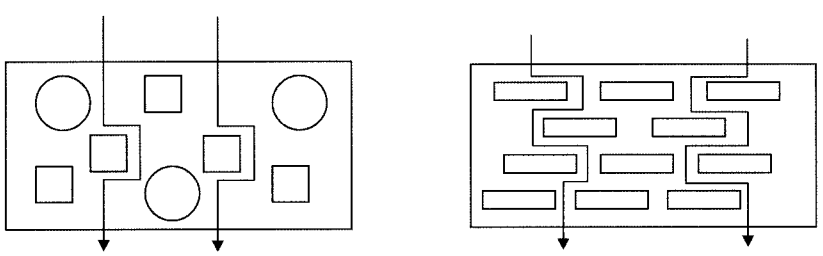

(A) Conventional filler reinforced composites (B) Polymer/ layered silicate nanocomposite

Fig. 7. Schematic illustration of formation of 'tortuous path' in nanocomposite. (A) conventional filler reinforced composites, (B) polymer/layered silicate nanocomposites.

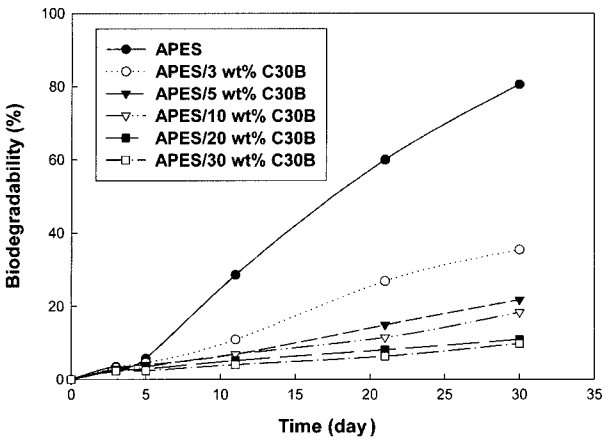

Fig. 8. Biodegradability of APES/Cloisite 30B nanocomposites with different clay content. (ref. 65)

attributed such seemingly contradictory result from the previously reported ones to the improved barrier properties of the nanocomposites developed by the intercalated clays with high aspect ratio, which hinder microorganism to diffuse in the bulk of the film through more tortuous paths. However, their explanation may not be probable since the molecular size of microorganisms is much greater than those of polymer and silicates used. Later, Rhim *et al.* (66) showed that a nanocomposite film made of the same organoclay (Cloisite 30B) has an antimicrobial activity due to the quarternary ammonium group in the organoclay. Consequently, the retarded biodegradability of APES/ Cloisite 30B nanocomposite was attributed to the antimicrobial action of the organoclay originated from the quarternary ammonium group. Such properties of antimicrobial action of the organoclay can be properly exploited for the development of nanocomposite food packaging materials with antimicrobial function.

Other properties Polymer nanocomposites also show significant improvement in other polymer properties useful for packaging application. For example, they have the transparency similar to pristine polymer materials because the clay platelets with about one nanometer thickness are well distributed through the polymer matrix. Thus, such clay platelets with size less than the wavelength of visible light do not hinder light's passage. Interestingly, the evenly distributed clay platelets well intercalated or exfoliated through the polymer matrix have a function of preventing transmission of UV light. Nanocomposite packaging materials with such optical properties (i.e., transparency and UV-barrier properties) can be utilized for transparent packaging materials or transparent barrier packaging films or coatings. Some examples include wrapping films and beverage containers, such as processed meats, cheese, confectionery, cereals, fruit juice, and dairy products, high barrier beer and carbonated drinks bottles, multi-layer films and containers, and barrier films and paper coatings.

Natural Biopolymer-based Nanocomposites

Numerous research works on polymer/clay nanocomposites have been performed. However, the matrices of polymer/ clay nanocomposites are mainly synthetic polymers including thermosets such as epoxy (67-69), thermoplastics such as poly(methyl methacrylate) (70, 71), non-polar polymers such as polyethylene (72-74) and polypropylene (75, 76), polar polymers such as nylon (77, 78), and conductive polymers such as polyaniline (79, 80). In addition, biodegradable plastics such as PLA (52, 62-64, 81, 82) and PCL (51, 83, 84) have been also tested for the processing of nanocomposites with layered silicate.

The literature available for natural biopolymer nanocomposite materials is quite limited and the materials prepared from natural polymers has poor performance compared with those prepared from synthetic polymers. However, recent research (85) has indicated that organoclays show much promise for starch-based polymer nanocomposites in terms of improvements in their mechanical properties and stability over those of the unfilled formulations.

Starch-based nanocomposites Starch is one of the natural biopolymers most widely used to develop environmentally-friendly packaging materials to substitute for petrochemical-based non-biodegradable plastic materials. Being an inherently biodegradable, renewable, and low-cost material, starch has high potential in food or non-food packaging applications. However, wide applications have been limited due to the lack of water barrier property and poor mechanical properties, such as film brittleness caused by high intermolecular forces.

Native starch is not a true thermoplastic but it can be converted into a plastic-like material called 'thermoplastic starch' (86). In the presence of plasticizers at high temperature (90-180°C) and under shear, starch readily melts and flows, allowing for its use as an injection, extrusion or blow molding material, similar to most conventional synthetic thermoplastic polymers. However, the pure thermoplastic starch still has the same limitations as native starch: it is mostly water-sensitive and has poor mechanical properties. In order to improve the properties, including the resistance to water and mechanical properties of starch plastics, reinforcement of starch with nano-scale minerals has been considered without interfering in the biodegradability of the composites (56, 63, 64).

De Carvalho *et al.* (87) prepared composites of thermoplastic starch and kaolin clay and tested their properties. They used corn starch (28% amylose) plasticized with glycerin (30 wt% of starch) and various amount of clay, i.e., 0, 10, 20, 30, 40, 50, and 60 phr (parts of kaolin per hundred parts of thermoplastic starch). Plate type composites (10×10 cm with 2.5 mm thickness) were formed through hot pressing the premixed sample at 160°C. Since scanning electron microscopy (SEM) images indicated that there were no smooth areas or large agglomerates, they concluded there was good kaolin dispersion throughout the composites. Both modulus (E) and tensile strength (TS) of the composites increased as the kaolin concentration increased up to 50 phr, then decreased, while the elongation (E_b) decreased almost monotonically. They found that the 50 phr composite seemed to represent the best composition for the materials, where E and TS showed increases of about 50 and 135%,

respectively, relative to the pristine starch matrix. They also found reinforcing starch with kaolin increased water resistance, which was pronounced until 20 phr. The glass transition temperatures (T_g) of the composites were slightly lower than that of unfilled starch matrix and the decrease was proportional to the amount of kaolin present in the composites. TG (thermogravimetry) analysis showed that all samples exhibited the same behavior of decomposition, i.e., the decomposition loss occurred at the same temperature and the residual weight was proportional to the kaolin content in the sample. This result is not consistent with the previously reported fact that thermal stability of polymer-clay composites usually increased (21, 25).

Park *et al.* (88) obtained well-ordered nanocomposites by the melt intercalation method with plasticized starch. They used potato starch plasticized with water and glycerol (starch/water/glycerol=5/2/3 by wt ratio) to make thermoplastic starch (TPS). TPS/clay hybrid with clay content of 5 wt% was formed through an injection molding at 110°C using a Mini-Max molder to get dog bone-shaped specimens. In their first study, they tested the effect of 4 kinds of MMT clays, i.e., one natural Na-MMT (Cloisite Na^+) and three organically modified MMT clays (Cloisite 30B, Cloisite 10A, and Cloisite 6A). XRD patterns of the hybrids with clay showed that the dispersion states of clays in the TPS matrix depended on the type of the clay used. It indicated the intercalation of TPS in the gallery of the silicate layer of the Cloisite Na^+, the minimum degree of intercalation with Cloisite 30B, and little or no intercalation of TPS with either Cloisite 10A or Cloisite 6A, which were also confirmed through TEM analysis. These results were attributed to the higher polymer clay compatibility and stronger polar-polar interactions in TPS/Na-MMT than the hybrids with other organoclays, where a modifier decreases the compatibility by making the clays hydrophobic to some extent. Among the clays tested by Park *et al.* (88), Cloisite 6A was most hydrophobic followed by Cloisite 10A, Cloisite 30B, and Cloisite Na^+. The hybrids of TPS/Cloisite Na^+ and TPS/Cloisite 30B exhibited higher tensile strength (TS) and elongation at break (E_b) due to the partial nanocomposite formation compared to 2 other hybrids. The TS and E_b of the TPS/Cloisite Na^+ hybrid increased by 30 and 20%, respectively, as compared to the pristine TPS. All the hybrid films showed lower water vapor permeability (WVP) than that of the pristine TPS. The water vapor barrier property was also affected by the degree of dispersion of clay. The WVP of TPS/Cloisite Na^+ was the lowest and that of TPS/Cloisite 10A was the highest. A significant increase in thermal stability was observed through TGA (thermogravimeric analysis) study when nanocomposites were formed by the melt intercalation method even at 5% filler content.

Park *et al.* (89) also tested the effect of filler concentration of TPS/clay hybrid with Cloisite Na^+ and Cloisite 30B with 2.5, 5, and 10% filler concentration. They confirmed their previous results that strong interaction between TPS and Cloisite Na^+ leads to the production of nanocomposites with better tensile and water vapor barrier properties than those of Cloisite 30B or the pristine TPS. They found both tensile and water vapor barrier properties are generally increased with increasing clay content. The effect on increase in such properties was remarkable up to 5% filler concentration, but the increases were not as significant above 5% filler concentration. In particular, they noticed the relative water vapor transmission rate of both hybrid films decreased exponentially with clay concentration, which is well agreed with the previously reported result of a polyimide-clay hybrid (58).

Wilhelm *et al.* (90) prepared nanocomposite films with glycerol-plasticized Cará starch (20% plasticizer to dry weight of starch) reinforced with Ca^{2+}-hectorite clay by the solution casting method. Clay mineral was filled with 5, 10, 15, 20, and 30% concentration of the plasticized starch. Degree of intercalation was found to be dependent on clay content in the starch/clay hybrid. XRD spectra revealed the decrease in interplanar distance with increase in clay content and the increase in *d*-space was inversely proportional to the amount of clay added. Dynamic mechanical analysis (DMA) results showed that storage modulus with the starch/clay hybrid films increased considerably at temperatures greater than 25°C, which is further evidence for the reinforcing effect of clay particles. Tensile test results showed that Young's modulus for the starch/clay hybrids increased with clay content, while maximum strain at break decreased. However, significant reinforcing effect was not observed below 20% clay content in the starch matrix. When clay content was increased to 30%, Young's modulus for the films increased significantly, being 72% higher than for non-filled films, but the maximum strain at break decreased to 5%. Though resilience of the starch/clay hybrid with 30% clay increased, it seemed to be too brittle for packaging applications. The content of plasticizer (20 wt% to starch) may not have been enough to make flexible films (87). TGA results indicated that the presence of clay did not generally affect the thermal stability of the hybrid films.

McGlashan and Halley (85) tested the use of nanoscale MMT in thermoplastic starch/polyester blends and found excellent improvements in film blowability and tensile properties. They also found an improvement in the clarity of the nanocomposite film, which was mainly attributed to disruption of large crystals.

Xu *et al.* (91) prepared starch acetate nanocomposite foam with four organoclays (Cloisite 30B, 10A, 25A, and 20A) by a melt intercalation method. Starch acetate (DS=1.78) was mixed with 5 wt% organoclays and 12 wt% ethanol in a mixer and the mixture was extruded in a twin screw extruder. XRD patterns of their composites clearly indicated that intercala-tion of starch acetate into the nanoclay layers occurred with all 4 clays. However, the degree of intercalation varied according to the nanoclay. For example, the degree of enlargement of the d_{001} spacing was the highest with Cloisite 30B (20.76 Å), followed by Cloisite 10A (18.21 Å), Cloisite 25A (15.97 Å), and Cloisite 20A (13.45 Å). As indicated by Park *et al.* (88), the intercalations between polymer and nanoclays were dependent on the compatibility and the surface polarities of polymer and organoclays. Hydrophobicities of the organic clays determined by the chemical structure were in the order of Cloisite 30B<10A <25A<20A. The addition of organoclays into a starch acetate matrix increased glass

transition temperature (T_g) by 6-14°C, depending on the type of clay. The increase in T_g with the addition of organoclay could be attributed to the formation of the intercalation structure. Intercalation of polymer into the clay galleries restricted the segmental movement of starch acetate and thus increased the T_g. The nanodispersion of starch acetate molecules in silicate layers also restricted their thermal motion, thus increased their thermal stability. The increase in thermal stability of the hybrid was reflected by the increase in the onset temperature of thermal degradation by 15-25°C with the incorporation of nanoclay into starch acetate. The intercalation also influenced the mechanical properties of the hybrid. The compressibility of starch acetate nano-composite significantly decreased relative to the unfilled starch acetate foam, while spring index was minimally influenced by the addition of nanoclays.

Recently, Huang and Yu (56) reported on preparation and properties of starch/MMT nanocomposites prepared with thermoplastic cornstarch and activated MMT by the melt intercalation method using an extruder with 8 wt% nanofiller loading. The thermoplastic cornstarch was obtained through plasticization of the starch with urea and ethanolamine, and the activated MMT was obtained using ethanolamine as the activating solvent. The XRD results indicated that the diffraction peak at 2θ of MMT was shifted from 8.75 to 7.06° through the activation of MMT with ethanolamine and that there was absence of a diffraction peak for the nanocomposite. The shift in peak angle for MMT implies that the activation of MMT with ethanolamine caused intercalation of the ethanolamine into the layers of MMT and enlarged the interlayer distance from 1.01 to 1.25 nm. The disappearance of the diffraction peaks for composites means that the crystal lattice structure of MMT was totally dispersed, and exfoliated nanocomposites were formed. TEM results also indicated that MMT layers were exfoliated and uniformly dispersed in starch matrix at the nanometer level. In addition to the increase in tensile properties (as shown in Fig. 5), the introduction of inorganic particles improved thermal stability of the starch/MMT nanocomposite as indicated by TGA analysis. The exfoliation of nanocomposite with 8% filler increased the onset temperature of decomposition from 271 to 279°C and decreased the mass loss before decomposition from 16.72 to 11.53%. Water resistance of the nanocomposites was also improved. The authors attributed such property improvement of the exfoliated nanocomposite starch to MMT possessing a high aspect ratio, and its homogeneous dispersion in a continuous polymer matrix.

Cellulose-based nanocomposites Cellulose is the most abundant naturally occurring biopolymer. It is composed of unbranched, linear chains of D-glucose molecules, linked to one another by 1,4-β-D glucosidic bonds. Since it is renewable, biodegradable, and biocompatible, cellulose has a high potential for being used for feedstock of biopackaging materials. Naturally, cellulose is a very highly crystalline, high molecular weight polymer, which is infusible in all but the most aggressive hydrogen bond-breaking solvents such as *N*-methylmorpholine-*N*-oxide. Because of its infusability, cellulose is usually converted into derivatives to make it more processable. Such derivatives include cellulose ethers such as methylcellulose (MC), carboxymethyl cellulose (CMC), hydroxypropyl cellulose (HPC), and hydroxypropyl methylcellulose (HPMC), and cellulose esters such as cellulose acetate (CA), cellulose acetate propionate (CAP), and cellulose acetate butyrate (CAB). Among the cellulose ethers, HPC is a true thermoplastic resin and is, therefore, capable of being extruded into films from the molten state (92). Cellulose acetate is currently used in high volume applications ranging from fibers, to films, to injection molding thermoplastics. Recently, interest in developing nanocomposites with cellulosic materials to obtain functional materials has been increased because of the improved mechanical and thermal properties and permeability of cellulose acetate films.

Park *et al.* (93) prepared green nanocomposites from cellulose acetate (CA) and organically modified clay. CA powder (DS=2.45) was plasticized with varying ratios of triethylene citrate (TEC) (CA/TEC=80:20, 70:30, and 60:40 by wt%), then the melt was compounded with 5 wt% of Cloisite 30B through extrusion at 160-220°C for 2-20 min and the melted hybrid was injection molded to obtain the desired nanocomposites. The XRD diffraction peak at 2θ shifted from 4.9° for pure nanoclay to 2.4° for nanocomposite prepared with 40% TEC plasticizer, which indicates significant intercalation and slight exfoliation in the hybrid structure. But no clear peak was observed for the nanocomposite with 20 and 30% TEC, which indicates partial exfoliation of organoclays in the CA/TEC matrix. The authors found that the extent of swelling of the clay (i.e., the degree of intercalation) increased with increase in plasticizer. However, highly intercalated organoclays with 30 or 40% of TEC were more difficult to exfoliate by external shear forces during extrusion processing than organoclays intercalated with 20% TEC. TEM images also showed that the nanocomposite prepared with 20% TEC obtained better exfoliation than those prepared with 30 or 40% TEC. The addition of clay nanoplatelets (5 wt%) increased the tensile modulus of the CA/TEC/Clay hybrids by 51, 31, and 110% for TEC contents of 20, 30, and 40%, respectively. DMA results showed that stiffness of the CA/TEC/clay hybrid, indicated by the storage modulus, increased with increased incorporation of clay, and both storage modulus and T_g of the hybrid decreased with increase in plasticizer content. Park *et al.* (93) asserted that the increase in storage modulus by reinforcement of the clay be attributed to the creation of a 3-dimensional interconnecting network of silicate layers, thereby strengthening the material through mechanical percolation. Addition of plasticizer increased the segmental motion in the CA backbone, thereby decreasing the stiffness and T_g. Water vapor permeability of CA films (film thickness = 250 μm), determined using Mocon Permatran, decreased up to 100% by reinforcing with organoclay.

The same researchers (94) prepared CA/organoclay nanocomposites with CA plasticized with TEC, organoclay (Cloisite 30B), and cellulose acetate butyrate grafted with maleic anhydride (CAB-*g*-MA) as the compatibilizer. They tested the effect of compatibilizer on the microstructure and mechanical properties of nanocomposites by varying the amount of compatibilizer included, i.e., 0, 5,

and 7.5 wt%. Morphology test results performed by atomic force microscopy (AFM), TEM, and XRD indicated that the addition of compatibilizer not only prevented formation of clay aggregate but also aided formation of exfoliation of clay platelets in the polymer matrix. Tensile and flexural properties showed that CA/TEC/clay nanocomposite with 5 wt% compatibilizer loading exhibited slightly higher values in TS, tensile modulus, flexural strength, and flexural modulus than those with 0 or 7.5% loading. They concluded that 5 wt% loading of compatibilizer is optimum for the best morphology and mechanical properties for the preparation of CA/TEC/clay composite.

Cho *et al.* (95) reported on the preparation and mechanical properties of nanocomposite film prepared with cellulose diacetate (CDA) and organoclay using a solvent intercalation method with a mixed solvent of methylene chloride and ethanol (9:1 w/w). First, they dissolved CDA (10 wt%) in the mixed solvent by mixing for about 4 hr, after which plasticizer was added. Then organoclay (Cloisite 25A) in varying amounts (1, 3, 5, and 7 wt%) was dispersed into the mixture through sonication for 2 hr. The solution was cast onto a silicon plate and dried at room temperature to obtain a clear and transparent film with thickness of about 200 μm. They confirmed the organoclay was distributed well in the CDA matrix using XRD patterns, which indicated that diffraction peaks observed in the organoclay powder at 4.16 and 19.72° (2θ) had disappeared in the nanocomposite films. They also found that T_g of the film decreased with increase in plasticizer content, and mechanical strength of the CDA film decreased by adding plasticizer, but the mechanical strength was recovered by incorporation of nanoclay.

Ruan *et al.* (96) reported interesting results on regenerated cellulose/tourmaline nanocrystal composite films. Tourmaline, a mixed stone, is a naturally complex group of hydrous silicate minerals containing Li, Al, B, and Si and various quantities of alkalis (K and Na) and metals (Fe, Mg, and Mn). Its structural formula is $Na(Li, Al)_3Al_6(BO_3)_3Si_6O_{18}(OHF)_4$. They prepared cellulose/tourmaline composite film using a solvent casting method. Cellulose and tourmaline were dissolved separately in aqueous solutions of 1.5 M NaOH/0.65 M thiourea (97), after which the tourmaline dispersion was mixed with the cellulose solution with sonication. The mixture was cast onto a glass plate and coagulated by immersing in a 5 wt% $CaCl_2$ aqueous solution and subsequently treated with a 3 wt% HCl aqueous solution. SEM images of both cellulose/tourmaline nanocomposite and unfilled cellulose films exhibited homogeneous structures suggesting that the hydrophilic NaOH/thiourea solution can effectively disperse the hydrophilic tourmaline nanocrystals and produce a homogeneous nanocomposite film. XRD patterns revealed that the crystals of tourmaline in the composite films were not changed, indicating that cellulose/tourmaline nanocomposite films maintained the structure and character of the tourmaline nanocrystals. Obviously, this is different from previously observed structures with nanocomposites using layered silicate nanoparticles. Nanoparticles like tourmaline can be classified as isodimensional nanoparticles where the three dimensions are in the order of nanometers, while the layered silicate nanoplatelets have only one dimension in the nanometer range (25). Unlike other nanocomposite films with layered silicates, tensile strength and T_g of the cellulose/tourmaline composite films were not increased with increase in filler content. On the contrary, they decreased a little bit. But the decrease in TS of the composite films with filler contents of 4-15% was not significant. This may be attributable to the fact that the hydroxyl group on cellulose is tightly bound to the tourmaline surface and results in good interfacial adhesion between cellulose and fillers. Interestingly, the cellulose/tourmaline composite films showed antimicrobial action against *Staphylococcus aureus*. This result implies potential use of the composites for functional packaging materials.

Another type of utilization of cellulose as nanocomposite feedstock is a cellulose whisker-reinforced nanocomposite. Cellulose whiskers (microcrystalline cellulose) have two dimensions in nanometer scale, like carbon nanotubes (25), and have been successfully used for the reinforcing of biopolymers. When starch matrix was filled with cellulose whiskers, a decrease in water sensitivity and increase in thermomechanical properties was observed (98). Though cellulose whisker reinforced bio-nanocomposites are 100% biodegradable, their effects on reinforcement are generally relatively very low. In addition, other problems are realized in commercial use of cellulose whiskers as structural materials (99) such as relatively high price and difficulty in dispersion of cellulose microfibrils in a polymer matrix. There are still significant scientific and technical challenges to the reinforcement of natural biopolymers with natural biopolymer-based materials, and research in this area is progressing that can be referred to for the further details (100-112).

Chitosan-based nanocomposites Chitosan is a partially deacetylated derivative of chitin, which is the second most abundant natural biopolymer next to cellulose. Structurally, chitosan is composed with glucosamine and N-acetyl-glucosamine units linked by the β-1-4-glucosidic bond. Because chitosan is biodegradable, nontoxic, and readily biocompatible, it has been studied extensively for various industrial and packaging applications. However, its properties as a packaging material also need to be improved, as do other hydrophilic natural biopolymer-based packaging materials. With regard to the present subject, only a few research works were found in the literature.

Lin *et al.* (113) reported on a novel method for the preparation of chitosan/montmorillonite nanocomposite using a solvent casting method. First they prepared potassium persulfate (KPS) intercalated MMT by dissolving purified MMT in 0.5% KSP and freeze-drying the mixture and pulverizing it to KPS-MMT powder (less than 75 μm). Chitosan solution (1 wt%) was prepared separately by dissolving chitosan (degree of deacetylation=85%) in 0.17 M acetic acid. As 5 phc (parts of MMT per hundred parts of chitosan by weight) KPS-MMT powder was added to the chitosan solution, the KPS instantly reacted with the chitosan, resulting in the cleavage of polymer chains and exfoliation of MMT as well. After removing the nonexfoliated MMT, solutions were cast to form a film of chitosan/MMT nanocomposite. The X-ray diffraction

pattern of KPS-MMT powder indicated that KPS had exchanged with the cations of MMT through the intercalation process when the MMT was treated with 0.5 CEC (cation exchange capacity) KPS. They recognized that the more KPS that was incorporated in the KPS-MMT, the greater the quantity of exfoliated MMT that was obtained, and that if MMT were not treated with KPS, it would not suspend in the acidic solution of chitosan. The TEM images of chitosan/KPS-MMT nanocomposite films showed that partially and fully exfoliated MMTs were observed with the layers flattened out in parallel to the surface. In the X-ray diffraction curve, the characteristic MMT peak observed at $2\theta = 6\text{-}7^{\circ}$ contributed by the c-axis of the layer structure was not detected in the composite films, suggesting that the MMT has been almost fully exfoliated. This was consistent with their results of TEM. The chitosan/KPS (0.5 CEC)-MMT nanocomposite film had higher tensile strength and lower Young's modulus than the pristine chitosan. Tensile properties of the nanocomposite films depended on the amount of KPS incorporated in the MMT. The higher the quantity of KPS incorporated into MMT used, the more MMT exfoliated along with the degradation of chitosan so that the Young's modulus increased but the tensile strength decreased. The nanocomposite also showed hindered degradation in *in vitro* testing with PBS (phosphate buffered saline) solution at 37°C.

Xu *et al.* (114) prepared chitosan-based nanocomposite films with Na-MMT and Cloisite 30B using a solvent casting method. Structural properties tested using XRD and TEM indicated that the nanoclay was exfoliated along with the chitosan matrix with small amounts of Na-MMT, and that intercalation with some exfoliation occurred with up to 5 wt% Na-MMT. However, microscale composite (tactoids) formed when Cloisite 30B was added to the chitosan matrix. They also confirmed that tensile strength of a chitosan film was enhanced and elongation at break decreased with addition of clay into the chitosan matrix.

Wang *et al.* (115) also prepared chitosan/MMT nanocomposite using the solvent intercalation method and found that an intercalated/exfoliated nanostructure was formed with low MMT content and an intercalated/flocculated nanostructure was formed with high MMT content. They also showed that the nano-dispersed clay improved the thermal stability and enhanced the hardness and elastic modulus of the matrix systematically with increases in clay loading. Recently, Rhim (116) also demonstrated that the mechanical and water vapor barrier properties of chitosan/MMT nanocomosite films were strongly affected by the clay concentration.

In addition, Darder *et al.* (117) prepared chitosan/MMT nanocomposite using a solution intercalation method with varying amounts of clay. The XRD patterns of pristine MMT, chitosan film, and corresponding nanocomposite films confirmed the intercalation of chitosan polymer in the silicate galleries, showing the decrease in 2θ values with increase in the ratio of chitosan/clay. Table 2 shows the d_{001} spacing and increase in d_{001} spacing of silicate galleries depending on the chitosan/clay ratio obtained from XRD patterns. Though they tested extraordinarily high amounts of clay (up to 400 wt% of chitosan), they found that the intercalation of the cationic biopolymer chitosan in Na-MMT provided compact and robust 3-dimensional nanocomposites with functional properties, which can be easily processed to construct bulk-modified electrodes.

Table 2. Change in d_{001} spacings of chitosan nanocomposite depending on the ratio of chitosan to montmorillonite (MMT)[1)]

Chitosan/clay ratio	d_{001} Spacings (nm)	Δd_{001} Spacings (nm)
Pristine MMT	1.20	-
0.25 : 1	1.39	0.19
0.5 : 1	1.45	0.25
1 : 1	1.69	0.49
2 : 1	2.00	0.8
5 : 1	2.04	0.84
10 : 1	2.09	0.89

[1)]Ref. 116.

Protein-based nanocomposites Composite soy protein with layered silicate clay materials has been tested to improve film properties. For example, Otaigbe and Adams (118) obtained better mechanical properties with improved water resistance for soy protein composites by blending with polyphosphate fillers. Rhim *et al.* (119) also demonstrated that soy protein isolate (SPI) films hybrid with organically modified MMT or bentonite increased tensile strength with improved water vapor permeability.

Dean and Yu (120) reported the effect of ultrasound treatment on inducing intercalation or exfoliation of unmodified Na-MMT (Cloisite Na^+) dissolved in water with or without glycerol. They used a Branson sonifier (model 250 W cell disruptor) with a maximum mechanical vibration frequency of 20 kHz to aid intercalation and exfoliation of the clay and plasticizers. Separate dispersions of clay/water and glycerol in clay/water were sonicated for varying times and the effects of the sonication treatment were observed through XRD measurements. An increase in the amount of intercalation of the clay/water solution was observed as the clay to water ratio decreased from 1:4 to 1:10. The degree of intercalation increased as the time of sonication increased. In the case of the clay/glycerol/water mixture, more than 25 min of sonication caused a complete exfoliation of the clay.

Dean and Yu (120) also prepared soy protein-based nanocomposite films and tested their microstructure and mechanical properties. They prepared the nanocomposite films by blending 400 g of water with 400 g of glycerol followed by adding 60 g of Cloisite Na^+, after which the mixture was treated with a point source ultrasonic device for one hour. This mixture was combined drip-wise to 1,200 g of soy protein isolate (Profam 974; Archer Daniels Midland, Decatur, IL, USA) using a high speed mixer for 5 min, then extruded using a twin screw extruder (Theysohn 30) at the set temperature of 140°C. They assessed the dispersion of clay through wide angle X-ray diffraction (WAXD) and TEM analysis. The XRD results showed that the characteristic peak for the neat Cloisite

Table 3. Tensile properties of neat soy protein isolate (SPI) film and nanocomposite films prepared with or without ultrasonic treatment[1)]

Film type	E (MPa)	TS (MPa)	E_b (%)
Neat SPI film	531±49	12.5±0.9	29.9±4.2
Nanocomposite without ultrasonic treatment	775±42	15.3±1.1	27.4±4.5
Nanocomposite with ultrasonic treatment	979±60	18.4±0.9	24.9±3.1

[1)]Means±SD; E, Young's modulus of elasticity; TS, tensile strength; E_b, elongation at break. (ref. 120)

Na^+ observed at 10 Å broadened and shifted to 60 Å in the nanocomposite prepared without ultrasonic treatment, indicating that the clay was partially intercalated or exfoliated. On the other hand, the diffractogram peak of clay (10 Å) disappeared in the nanocomposite prepared with ultrasonic treatment, indicating the nanocomposite formed was exfoliated.

The TEM images of both nanocomposites confirmed the XRD data. A large agglomerate along with smaller tactoids of silicates were observed in the nanocomposite prepared without ultrasound treatment, while mostly single exfoliated silicates were observed in the nanocomposite prepared with ultrasound treatment. Glass transition temperature (T_g) determined by both DMA and differential scanning calorimetry (DSC) increased in both nanocomposites; Dean and Yu (120) postulated that this was due to the restriction in molecular motion of the protein by the dispersion of the nanoclay. The effects of nanocomposite formation are reflected in the mechanical properties of the resultant films (Table 3). The most significant improvement observed in the mechanical properties was for the elastic modulus; in particular, an increase of 84% in modulus of the ultrasonically treated nanocomposite films was observed compared with neat protein film. Nanocomposite films both without and with ultrasonic treatment increased in tensile strength, by 23 and 47%, respectively. The elongation at break for both nanocomposites was reduced due to the inclusion of a brittle silicate into a polymer.

Though Dean and Yu (120) demonstrated mechanical properties of SPI films improved by hybridizing with nanoclay, they did not measure water barrier properties of the composite. Rhim *et al.* (119) prepared composite films of SPI and various clays such as organically modified MMT (O-MMT) (Nanomer I.34TCN; Nanocor Inc., Arlington Heights, IL, USA), bentonite (OPZIL AOK; SÜD-CHEMIE Korea, Pohang, Korea), talc powder (magnesium silicate hydrous, $3MgO{\cdot}4SiO_2{\cdot}H_2O$), and zeolite. Each composite film solution was prepared by adding 0.5 g of one of the clay mineral samples into 100 mL distilled water with 2 g glycerol; then the mixture was vigorously stirred for 30 min and sonicated for 10 min. Five g of SPI was then dissolved into the suspension and heated for 20 min at 90°C in a water bath. The solution was cast onto a leveled Teflon-coated glass plate and dried at room temperature. Neat SPI films were prepared with the same method without adding clay. Rhim *et al.* (119) tested the effect of compositing between SPI and clays by measuring the mechanical and water barrier properties of the films without testing the microstructure of the films using XRD or TEM. As shown in Table 4 and 5, mechanical and water barrier properties of the SPI films were significantly affected by the filler materials used. Tensile strength of the SPI hybrid films with O-MMT and bentonite, which are composed of mostly layered silicate clays, increased significantly up to 30%, while those with talc and zeolite, which are particle type fillers, decreased. As expected, the resilience of all the hybrid SPI films decreased due to the restriction of molecular motion of polymer caused by the composition of brittle clays. The enhancement in TS of SPI films hybrid with O-MMT and bentonite may be attributed to the reinforcement provided by the intercalation of SPI in these clay minerals, as well as a fine dispersion of the particles in the SPI matrix.

Generally, compositing with clay minerals induced a decrease in WVP of SPI films ranging from 7 to 52% depending on the clay minerals used (Table 5). It is noteworthy that the water vapor barrier property of SPI films hybrid with bentonite increased two-fold compared to that of the neat SPI film. This result further indicates that some specific structure, such as intercalation of SPI in clays, was developed in the films composited with clay minerals particularly with bentonite.

The observed decrease in WVP is of great importance in evaluating the composites for use in food packaging, protective coatings, and other applications where efficient

Table 4. Tensile strength (TS) and elongation at break (E_b) of soy protein isolate (SPI) and clay-based nanocomposite films[1)]

Film type	Thickness (μm)	TS (MPa)	E_b (%)
Neat SPI	105.3 ± 16.6^{ab}	7.5 ± 1.0^{d}	17.5 ± 3.2^{bcd}
O-MMT[2)]/SPI	103.2 ± 5.2^{ab}	9.4 ± 2.5^{e}	11.5 ± 2.0^{ab}
Bentonite/SPI	99.6 ± 5.1^{a}	9.7 ± 0.3^{e}	14.8 ± 5.1^{bcd}
Talc/SPI	105.0 ± 1.3^{ab}	6.8 ± 0.3^{bcd}	12.1 ± 3.0^{bc}
Zeolite/SPI	116.7 ± 6.9^{bc}	4.6 ± 0.4^{a}	12.7 ± 0.4^{bcd}

[1)]Means of three replicates±SD; Any 2 means in the same column followed by the same letter are not significantly ($p>0.05$) different by Duncan's multiple range tests. (ref. 119)
[2)]Organically modified montmorillonite.

Table 5. Water vapor permeability (WVP) and water solubility (WS) of soy protein (SPI)- and clay-based nanocomposite films[1)]

Film type	MC (%, wb)	WVP ($ng{\cdot}m/m^2{\cdot}sec{\cdot}Pa$)	WS (%)
Neat SPI	19.3 ± 1.2^{ab}	3.1 ± 0.2^{efg}	27.8 ± 4.3^{e}
O-MMT[2)]/SPI	19.6 ± 0.9^{abc}	2.9 ± 0.6^{ef}	12.3 ± 4.8^{a}
Bentonite/SPI	19.0 ± 0.9^{a}	1.5 ± 0.5^{a}	13.7 ± 0.3^{ab}
Talc/SPI	20.5 ± 0.3^{abc}	2.3 ± 0.1^{bcd}	21.2 ± 4.0^{cd}
Zeolite/SPI	20.9 ± 0.6^{abc}	2.0 ± 0.1^{b}	13.5 ± 4.0^{ab}

[1)]Means of 3 replicates±SD; Any 2 means in the same column followed by the same letter are not significantly ($p>0.05$) different by Duncan's multiple range test. (ref. 119)
[2)]Organically modified montmorillonite.

polymer barrier properties are needed. For these applications, significant reduction in WVP can result in either increased barrier efficiency, or reduced thickness of the barrier layer for the same efficiency. Compositing with clay minerals improved the water resistance properties of the SPI films as evidenced by decreases in WS (water solubility) values (Table 5). The increase in water resistance may also have been due to the development of a polymeric composite structure with clay minerals.

Gelatin, an animal protein, was also tested for the preparation of a bionanocomposite with MMT clay in order to improve mechanical and water resistance properties of the polymer (121). Zheng *et al.* (121) prepared gelatin/MMT nanocomposite using a solution intercalation method. Gelatin (type B, extracted from bovine skin) solution was prepared separately by dissolving gelatin in deionized water heated to 70°C, and the solution was added into 2 wt% ultrasonically pretreated MMT suspension under vigorous stirring at 70°C. Then the mixture was cast on a mold. XRD results indicated that an intercalated or partially exfoliated nanocomposite was formed. The tensile strength and Young's modulus were improved notably (up to 60 and 80%, respectively), which varied with MMT content as well as pH of the gelatin matrix. The wet mechanical strength was also significantly improved in the nanocomposite, which was mainly attributed to nanodispersion of MMT in the gelatin matrix and the barrier effect of MMT sheets to solvent molecules.

Potential Application in an Active Food Packaging

The use of proper packaging materials and methods to minimize food losses and provide safe and wholesome food products has always been the focus of food packaging. In addition, consumer trends for better quality, fresh-like, and convenient food products have intensified during the last decades. Therefore, a variety of active packaging technologies have been developed to provide better quality, wholesome and safe foods and also to limit package-related environmental pollution and disposal problems (122). Active packaging is a type of packaging that changes the condition of the packaging to extend shelf-life or improve safety or sensory properties while maintaining quality of the food (123).

As one of the innovative active packaging methods, antimicrobial packaging, applying antimicrobial compounds in combination with food packaging materials, has been receiving considerable attention as a potential application for a variety of foods including meat, fish, poultry, bread, cheese, fruits, and vegetables (124-126). The potential application of these films with antimicrobial activities would allow surface contact with food that could help control growth of pathogenic and spoilage microorganisms.

Various antimicrobial agents have been proposed and/or tested for this purpose, including organic acids such as sorbate, propionate, and benzoate (127) or their respective acid anhydrides (128), bacteriocins, e.g., nisin and pediocin (129), enzymes such as lysozyme (130), metals (131) and fungicides such as benomyl (132) and imazalil (133). The active component of these antimicrobial systems can be either organic or inorganic. In particular, the inorganic systems are based on metal ions such as silver, copper, and platinum. Silver ions as an antimicrobial are ideally suited for a wide range of applications: appliances, building products, medical devices, water filtration, delivery systems, and obviously, food processing and packaging (134). Ag-substituted zeolite is the most common antimicrobial agent incorporated into plastics. Ag-ions, which inhibit a range of metabolic enzymes, have strong antimicrobial activity. The unique feature of Ag-zeolites is their broad antimicrobial spectrum. As Ag-zeolite is expensive, it is laminated as a thin layer (3-6 μm) containing Ag-zeolite. The normal incorporation level varies from 1 to 3% (131).

The mode of application of antimicrobial agents in food systems is critical for success. Incorporation of antimicrobial agents or growth inhibitors into food formulations may result in partial inactivation of the active substances by product constituents and is therefore expected to have only limited effect on surface flora (135, 136). Also, direct application of antimicrobial agents onto food surfaces, by dipping or spraying, has been shown to be inefficient, due to the rapid diffusion of the active substances within the bulk of food (136, 137). The use of packaging film based on an antimicrobial polymer could prove more efficient, by maintaining high concentrations on the food surface with a low migration of active substance (136-138).

The choice of the antimicrobial, however, is often limited by the incompatibility of the component with the packaging material or by the heat lability of the component during extrusion (127, 139). This explains the importance of choice for proper biopolymer matrix and antimicrobial agents as well as other ingredients such as plasticizer and compatibilizer. Because of the characteristic inhibitory mechanism and the specific activity of each antimicrobial agent against a specific microorganism, the antimicrobial films have a limited antimicrobial spectrum. Combining two or more antimicrobials can widen this limited spectrum.

Taking into account its potential antimicrobial activity and good film forming ability, chitosan seems to be an ideal antimicrobial film preparation material (137, 138, 140-144). Chitosan is the deacetylated derivative of chitin (β-[1-4]-poly-N-acetyl-D-glucosamine), one of the most abundant natural polymers obtained as a by-product of seafood processing. Chitosan has antimicrobial activities against a wide variety of microorganisms including fungi, algae, and some bacteria (145). Furthermore it is inexpensive, nontoxic, biodegradable, and biocompatible. Chitosan is a renewable and non-toxic biopolymer with excellent biocompatibility with other substances. Inherent antimicrobial properties of chitosan and its high film-forming and entrapping ability could be the primary driving force in the development of new applications for this underused biopolymer.

There are some limitations to the application of chitosan film for packaging, because of its high sensitivity to moisture. One strategy to overcome this drawback is to associate chitosan with a moisture resistant polymer, which would maintain the overall biodegradability of the product. Associations between polymers can be blends or multilayer products (for example, coating or laminating), but blending is easier and a more effective way to prepare multiphase polymeric materials with desirable properties.

Blending chitosan with other biodegradable polymers,

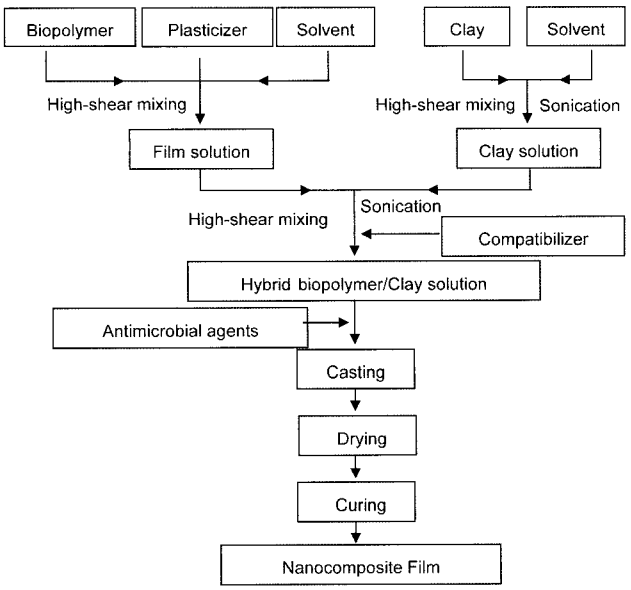

Fig. 9. Flow diagram for the preparation of antimicrobial biopolymer-based nanocomposite films using a solvent casting method.

for example, poly(3-hydroxybutyric acid) (PHB) (146), PCL (147, 148), and PLA (149) has been used to modify chitosan's water sensitivity properties.

An ideal solution to food industry concerns about environmental pollution and food safety would be development of biopolymer-based antimicrobial films by incorporating food-grade antimicrobials into biopolymer films. A composite antimicrobial nanocomposite film is particularly desirable due to its acceptable structural integrity and barrier properties imparted by the nanocomposite matrix, and the antimicrobial properties contributed by the natural antimicrobial agents impregnated within. In addition, such nanocomposite films prepared based upon natural biopolymers are environmentally-friendly with all the benefits expected from both biopolymer and nanocomposite packaging materials.

In order to fully realize the benefits of natural biopolymer/clay nanocomposites, it is necessary that the clay particles become fully exfoliated and uniformly dispersed in the polymer matrix. For the preparation of the natural biopolymer-based nanocomposite films with antimicrobial activity, a solvent casting method can be properly used as shown in Fig. 9. First, polymer and clay solutions are prepared separately. The biopolymer is dissolved in a solvent with high-shear mixing as the first step in the preparation of natural biopolymer films using a solvent casting method. A clay solution is prepared by initially swelling and dispersing of layered nanoclay particles in the same solvent as that used for film-forming solution. To achieve intercalation of the solvent into the stacked layers, the mixture is subjected to high-shear mixing and to ultrasonic treatment (43, 71, 120, 150). In the second step of the process, the clay solution is added to the polymer solution in a dropwise fashion and the resulting mixture is subjected to high-shear mixing and ultrasonic treatment again. The functionally active materials (such as antimicrobial agents) are added into the mixture and cast onto a glass plate. The solution is allowed to dry in ambient or elevated temperature conditions to make a free-standing film, then further dried or cured if needed. In this process, intercalation or exfoliation of nanoclay particles in a polymer matrix is a most important step for preparation of the nanocomposite films, as well as selection of the most compatible materials for the film preparation (such as nanoclay, biopolymer, antimicrobial agents, and plasticizer).

Recently, Rhim *et al.* (66) prepared chitosan-based nanocomposite films using a solvent casting method based on the procedure depicted in Fig. 9 to test the effect of nanoclay or particles such as Cloisite 30B, Na-MMT, Nano-silver, and Ag-Ion on the mechanical and water vapor barrier properties as well as antimicrobial activities of the resulting films. Chitosan film solution was prepared by dissolving 2%(w/v) chitosan in a 1% acetic acid solution with 25% of glycerol (w/w, relative to chitosan on a dry basis). In addition, 4 types of nanocomposite films were prepared by using 5% of each type of nanoparticle (w/w, relative to chitosan on a dry basis). Figure 10 shows XRD patterns of 4 types of nanocomposite films. XRD results indicated that a certain degree of intercalation occurred in the case of layered silicate nanoparticles like Na-MMT and Cloisite 30B, but more intercalation was observed in the chitosan/Na-MMT nanocomposite films. Table 6 and 7 show tensile and water barrier properties of chitosan-based nanocomposite films. Except for the nano-silver films, which are dark gray in surface color, apparent color and transparency of the nanocomopsite films were not significantly different from the control chitosan film. Dispersing nanoparticles into chitosan polymer matrix increased tensile strength significantly and decreased WVP significantly. Antimicrobial activity of the nanocomposite films was tested against 2 Gram-positive bacteria, *S. aureus* and *Listeria monocytogenes*, and 2 Gram-negative bacteria, *Salmonella typhimurium* and *Escherichia coli* O157:H7 using both disk method and viable cell count method. Results of disk method (Table 8) indicated no clear microbial inhibition zone with chitosan/Na-MMT nanocomposite films, while Nano-silver- and Ag-Ion-incorporated nanocomposite films exhibited distinctive microbial inhibition zones against both Gram-positive and Gram-negative bacteria. Interestingly, Cloisite 30B-

Table 6. Tensile properties of chitosan-based nanocomoposite films[1)]

Film type	Thickness (μm)	TS (MPa)	E_b (%)	E (MPa)
Neat chitosan	64.0±6.0^a	32.9±0.7^b	54.6±3.0^{ab}	135.6±25.0^b
Na-MMT	70.0±9.2^a	35.1±0.9^{ab}	50.3±11.7^{bc}	191.3±81.2^b
Cloisite 30B	63.3±2.3^a	36.8±3.3^{ab}	66.3±5.3^a	184.6±51.9^b
Nano-silver	64.7±9.0^a	35.9±1.9^{ab}	46.3±7.6^{bc}	259.2±161.3^b
Ag-ion	61.3±5.0^a	38.0±3.4^a	38.9±1.4^c	455.4±22.1^a

[1)]Means of three replicates±SD; Any 2 means in the same column followed by the same letter are not significantly different (p>0.05) by Duncan's multiple range test. TS, tensile strength; E_b, elongation at break; E, Young's modulus of elasticity; MMT, montmorillonite. (ref. 66)

Table 7. Water vapor barrier and water resistance properties of chitosan-based nanocomposite films[1)]

Film type	MC (%, w.b.)	WVP ($\times 10^{-12}$ kg·m/m^2·sec·Pa)	RH_I (%)	CA (degrees)	WS (%)
Neat chitosan	27.1±0.8^a	1.31±0.07^a	76.2±1.4^c	45.6±0.2^c	13.6±1.1^b
Na-MMT	26.4±0.4^a	0.98±0.15^{bc}	78.8±0.6^a	47.4±0.2^b	12.5±0.8^b
Cloisite 30B	24.3±0.2^b	0.92±0.03^c	78.2±0.2^{ab}	43.4±1.3^d	13.2±1.0^b
Nano-silver	24.5±0.0^b	0.95±0.12^{bc}	78.1±0.2^{ab}	48.5±1.1^b	14.1±0.8^{ab}
Ag-ion	22.3±0.3^c	0.96±0.05^{bc}	77.3±0.4^{bc}	50.4±1.0^a	15.4±0.6^a

[1)]Means of three replicates±SD; Any 2 means in the same column followed by the same letter are not significantly different (p>0.05) by Duncan's multiple range test. MC, moisture content; WVP, water vapor permeability; RH, actual relative humidity value underneath the film covering the WVP measuring cup; CA, contact angle of water drop; WS, water solubility; MMT, montmorillonite. (ref. 66)

Table 8. Antimicrobial activity[1)] of the chitosan nanocomposite films as observed by an agar diffusion assay on plate medium[2)]

Test organisms	Film type					
	Neat chitosan	Na-MMT	Cloisite 30B	Nano-silver	Ag-ion$_5$[3)]	Ag-ion$_{20}$[3)]
S. aureus ATCC-14458	-	-	++	+	+	+
L. monocytogenes ATCC-19111	-	-	+	+	+	++
S. typhimurium ATCC-14028	-	-	-	+	+	++
E. coli O157:H7 ATCC-11775	-	-	-	+	+	++

[1)]-, no inhibition; +, clear zone of 6-8 mm; ++, clear zone of 8-10 mm.
[2)]Culture medium, TSA(tryptic soy agar, Difco Lab.), incubation temperature, 37°C.
[3)]Ag-ion$_5$, Ag-ion$_{20}$: Ag-ion concentration, 5 and 20% (w/w of chitosan), respectively. (ref. 66)

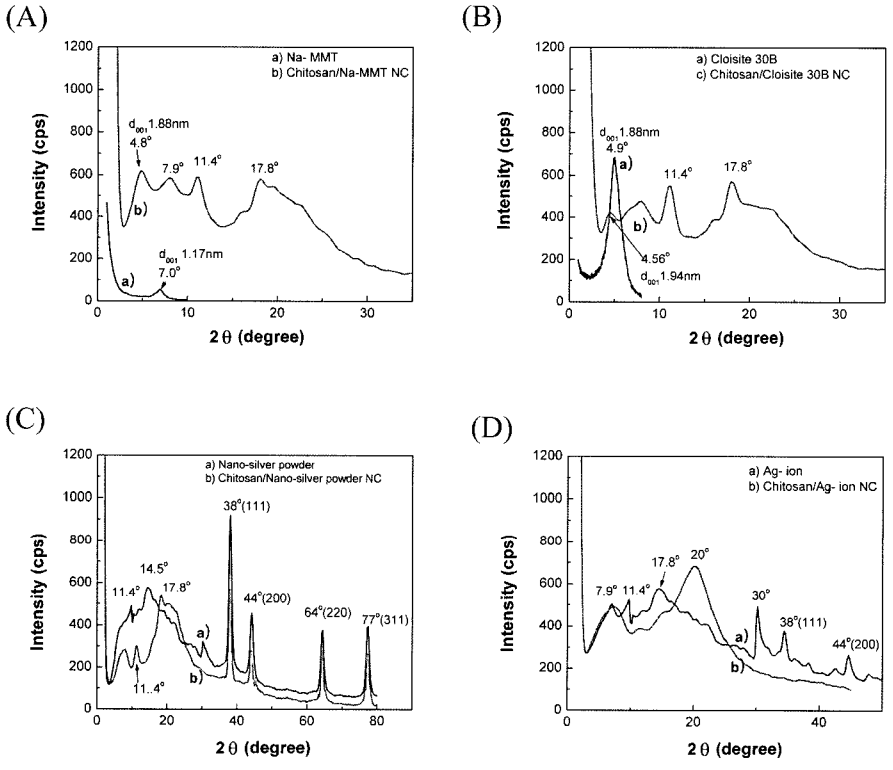

Fig. 10. X-ray diffraction patterns of chitosan film, nanofillers, and their nanocomposite (NC) films. (A) chitosan/Na-montmorillonite, (B) chitosan/Cloisite 30B, (C) chitosan/nanosilver powder, and (D) chitosan/Ag-ion nanocomposites. (ref. 66)

incorporated nanocomposite films exhibited antimicrobial activity against Gram-positive bacteria, *S. aureus* and *L. monocytogenes*. This result was confirmed with the viable cell count method as shown in Fig. 11. Since silver ions are well known to have antimicrobial activity against wide range of microorganisms (134), it was expected that silver-

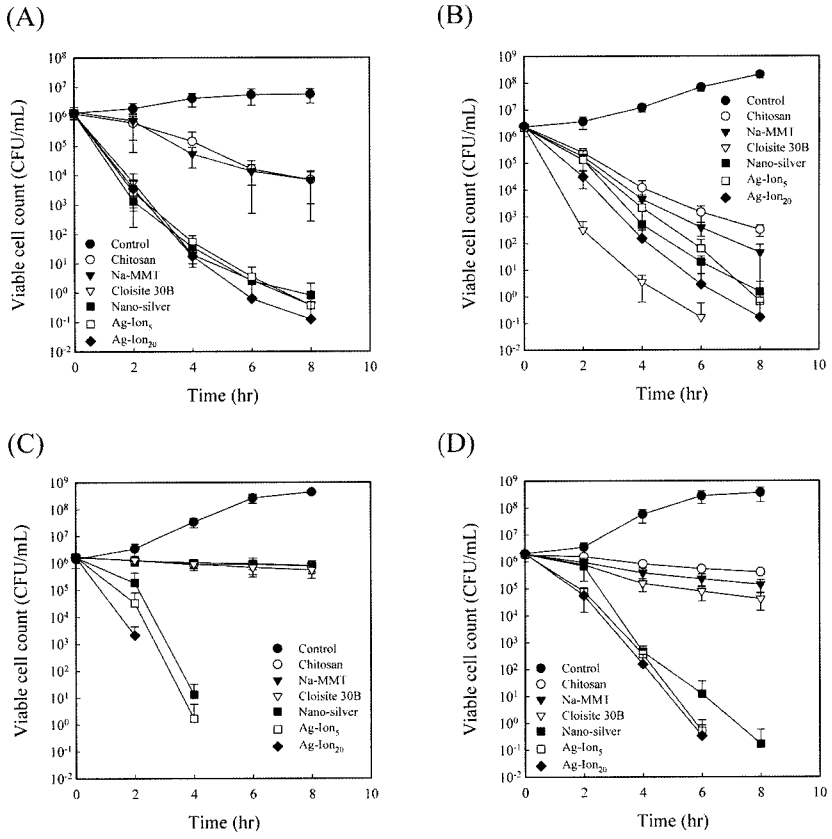

Fig. 11. Antimicrobial activity of chitosan-based nanocomposite films against (A) *S. aureus*, (B) *L. monocytogenes*, (C) *S. typhimurium*, and (D) *E. coli* O157:H7. (ref. 66)

containing nanocomposite films exhibit antimicrobial action. However, the antimicrobial activity of Cloisite 30B-incorporated nanocomposite films has been observed for the first time. Rhim *et al.* (66) attributed this to the antimicrobial activity of the quarternary ammonium group in the silicate layer incorporated to the organoclay (Cloisite 30B) through organophilic modification. The effectiveness of such quarternary ammonium group for disrupting bacterial cell membranes and causing cell lysis has been well known (151-154). Wang *et al.* (155) also reported a similar result with chitosan-based nanocomposite films composited with layered silicate, rectorite, which was organically modified with cetyltrimethyl ammonium bromide. They found the nanocomposite films exhibited excellent inhibition effect on Gram-positive bacteria, *S. aureus* and *Bacillus subtilis*, whereas they only exhibited slight antimicrobial activity against Gram-negative bacteria, *E. coli* and *Pseudomonas aeruginosa*. They also found that the minimum inhibition concentration (MIC) values of the nanocomposite films was 4-30 times lower than that of chitosan film depending on the nanoclay content. They suggested that the antimicrobial action of the nanocomposite films could be attributed to the positively charged amino groups of chitosan molecule interacting with the predominantly anionic molecules at the cell surface. This interaction could change the permeability of cell membrane of the microorganisms, resulting in a leakage of intercellular components, and caused the death of the cell. In addition, they also attributed to the adsorption and immobilization of bacteria by the clay with large surface area. However, their explanation on the antimicrobial action of the chitosan film is controversial, because antimicrobial action of chitosan film is dependent on the molecular weight of chitosan used. It is well known that chitosans with high molecular weight used for the preparation of chitosan films is not expected to show antimicrobial action. The antimicrobial action of the chitosan-based nanocomposite films may be attributed to the organic acid used for the solvent and the functional group of cetyltrimethyl ammonium bromide in the rectorite used for the preparation of the nanocomposite film (66).

All of these results indicate high potential for antimicrobial bio-nanocomposite films with improved mechanical and barrier properties for use in active packaging applications.

Conclusions

Natural biopolymer-based biodegradable packaging materials are a new generation of polymers emerging on the packaging market. Biodegradable packaging materials have an expanding range of potential applications and, driven by the growing use of plastics in packaging and the perception that biodegradable plastics are 'environmentally-friendly', their use is predicted to increase. Many consumer plastic products may be replaced by the natural

biopolymer-based plastics, which may be used for disposable plastic bags, cups, plates, containers and utensils, and other plastic products. However, due to the inherent properties of the natural biopolymer packaging materials such as lower mechanical strength and lower water resistance than their petroleum-based counterparts, they have not been widely used in the food packaging industry. The application of nanotechnology might provide one possible solution for this problem.

Several examples of natural biopolymers, with or without further modification, for the preparation of nanocomposites with nano-sized clays have been discussed. Even though limited numbers of research studies on natural biopolymer-based nanocomposites are available, bio-nanocomposites prepared with natural biopolymers, such as starch, cellulose, and protein, increased mechanical properties and decreased water sensitivity without sacrificing biodegradability. Such property improvements are generally attained at low nanoclay content (less than 5%) compared to that of conventional fillers (in the range of 10 to 50%). For these reasons, nanocomposites are far lighter in weight than conventional composite materials, making them competitive with other materials for specific applications such as in packaging.

Bio-nanocomposites have very strong future prospects, though the present low level of production and high cost restrict them from a wide range of applications. In spite of improvements in mechanical and water barrier properties of several natural biopolymers through nanocomposition technology, these improvements are not sufficient for petroleum-based plastics to be replaced. In particular, water resistance is too poor to utilize the bio-nanocomposites as packaging materials, especially in wet environmental conditions. Therefore, the most important factors for the development of new packaging materials using natural biopolymer-based nanocomposites include development of the optimum formulation for the individual polymer and processing method to obtain desired properties to meet a wide range of applications as well as cost reduction of the bio-nanocomposites.

There is huge potential for the natural polymer-based nanocomposites to enhance quality and safety of packaged foods by increasing barrier properties of packaging materials with antimicrobial activity. Natural biopolymer-based nanocomposite packaging materials appear to have a very bright future for a wide range of applications in the food industry including innovative active food packaging with bio-functional properties. However, a natural biopolymer-based nanocomposite film material with the active packaging function is in its infancy and is now emerging because of environmental concerns and expectations for high quality food products. Much research work on the preparation and application of bio-nanocomposite packaging with functional properties is expected for such biodegradable nanocomposite materials to replace or reduce the use of the existing petrochemical-based packaging materials available.

References

1. Han JH, Gennadios A. Edible films and coatings: A review. pp. 239-262. In: Innovations in Food Packaging. Han JH (ed). Elsevier Academic Press, San Diego, CA, USA (2005)
2. Petersen K, Nielsen PV, Bertelsen G, Lawther M, Olsen MB, Nilsson NH, Mortensen G. Potential of biobased materials for food packaging. Trends Food Sci. Tech. 10: 52-68 (1999)
3. Guilbert S, Gontard N, Gorris LGM. Prolongation of the shelf life of perishable food products using biodegradable films and coatings. Lebensm.-Wiss. Technol. 29: 10-17 (1996)
4. Krochta JM, De Mulder-Johnston C. Edible and biodegradable polymer films: Challenges and opportunities. Food Technol.-Chicago 51: 61-74 (1997)
5. Debeaufort F, Quezada-Gallo JA, Voilley A. Edible films and coatings: Tomorrow's packagings: A review. Crit. Rev. Food Sci. 38: 299-313 (1998)
6. Wong DWS, Camirand WM, Pavlath AE. Development of edible coatings for minimally processed fruits and vegetables. pp. 65-88. In: Edible Coatings and Films to Improve Food Quality. Krochta JM, Baldwin EA, Nisperos-Carriedo MO (eds). Technomic Publishing Company, Inc., Lancaster, PA, USA (1994)
7. Baldwin EA. Edible coatings for fresh fruits and vegetables: Past, present, and future. pp. 25-64. In: Edible Coatings and Films to Improve Food Quality. Krochta JM, Baldwin EA, Nisperos-Carriedo MO (eds). Technomic Publishing Company, Inc., Lancaster, PA, USA (1994)
8. Han JH. Antimicrobial food packaging. Food Technol.-Chicago 54: 56-65 (2000)
9. Avena-Bustillos RJ, Krochta JM. Water vapor permeability of caseinate-based edible films as affected by pH, calcium crosslinking, and lipid content. J. Food Sci. 58: 904-907 (1993)
10. Gontard N, Duchez C, Cuq JL, Guilbert S. Edible composite films of wheat gluten and lipids: Water vapor permeability and other physical properties. Int. J. Food Sci. Tech. 29: 39-50 (1994)
11. Rhim JW. Physical and mechanical properties of water resistant sodium alginate films. Lebensm.-Wiss. Technol. 37: 323-330 (2004)
12. Rhim JW, Gennadios A, Handa A, Weller CL, Hanna MA. Solubility, tensile, and color properties of modified soy protein isolate films. J. Agr. Food Chem. 48: 4937-4931 (2000)
13. Rhim JW, Weller CL. Properties of formaldehyde adsorbed soy protein isolate films. Food Sci. Biotechnol. 9: 228-233 (2000)
14. Micard V, Belamri R, Morel HM, Guilbert S. Properties of chemically and physically treated wheat gluten films. J. Agr. Food Chem. 48: 2948-2953 (2000)
15. Rhim JW, Wu Y, Weller CL, Schnef M. Physical characteristics of a composite film of soy protein isolate and propyleneglycol alginate. J. Food Sci. 64: 149-152 (1999)
16. Gennadios A, Rhim JW, Handa A, Weller CL, Hanna MA. Ultraviolet radiation affects physical and molecular properties of soy protein films. J. Food Sci. 63: 225-228 (1998)
17. Rhim JW, Gennadios A, Weller CL, Cezeirat C, Hanna MA. Soy protein isolate-dialdehyde starch films. Ind. Crop Prod. 8: 195-203 (1998)
18. Ghorpade VM, Li H, Gennadios A, Hanna MA. Chemically modified soy protein films. T. ASAE 38: 1805-1808 (1995)
19. Park HJ, Weller CL, Vergano PJ, Testin RF. Permeability and mechanical properties of cellulose-based edible films. J. Food Sci. 59: 1361-1370 (1993)
20. Gennadios A, Brandenburg AH, Weller CL, Testin RF. Effects of pH on properties of wheat gluten and soy protein isolate films. J. Agr. Food Chem. 41: 1935-1939 (1993)
21. Sinha Ray S, Okamoto M. Polymer/layered silicate nanocomposites: a review from preparation to processing. Prog. Polym. Sci. 28: 1539-1641 (2003)
22. Vaia RA, Gianelis EP. Lattice model of polymer melt intercalation in organically-modified layered silicates. Macromolecules 30: 7990-7999 (1997)
23. Giannelis EP. Polymer layered silicate nanocomposites. Adv. Mater. 8: 29-35 (1996)
24. Pandey JK, Kumar AP, Misra M, Mohanty AK, Drzal LT, Singh RP. Recent advances in biodegradable nanocomposites. J. Nanosci. Nanotechno. 5: 497-526 (2005)
25. Alexandre M, Dubois P. Polymer-layered silicate nanocomposites: Preparation, properties, and use of a new class of materials. Mater. Sci. Eng. 28: 1-63 (2000)

26. Yu YH, Lin CY, Yeh JM, Lin WH. Preparation and properties of poly(vinyl alcohol)-clay nanocomposite materials. Polymer 44: 3553-3560 (2003)
27. Schmidt D, Shah D, Giannelis EP. New advances in polymer/layered silicate nanocomposites. Curr. Opin. Solid St. M. 6: 205-212 (2002)
28. Hernandez RJ, Selke SEM, Culter JD. Additives and compounding. pp. 135-156. In: Plastics Packaging. Hanser Publishers, Munich, Germany (2000)
29. Giannelis EP. Polymer-layered silicate nanocomposites: Synthesis, properties, and applications. Appl. Organmet. Chem. 12: 675-680 (1998)
30. Okada A, Kawasumi M, Usuki A, Kojima Y, Kurauchi T, Kamigaito O. Nylon-6-clay hybrid. Mat. Res. Soc. Symp. P. 171: 45-50 (1990)
31. Sinha Ray S, Bousmina M. Biodegradable polymers and their layered silicate nanocomposites: In greening the 21st century materials world. Prog. Mater. Sci. 50: 962-1079 (2005)
32. Sinha Ray S, Biswas M. Recent progress in synthesis and evaluation of polymer-montmorillonite nanocomposites. Adv. Polym. Sci. 155: 167-221 (2001)
33. Carrado KA. Synthetic organo- and polymer-clays: preparation, characterization, and materials applications. Appl. Clay Sci. 17: 1-23 (2000)
34. Fischer S, Vlieger J, Batenburg L, Fischer H, Kock T. 'Green' nanocomposite materials - New possibilities for bioplastics. Materialen 16: 3-7, 12 (2000)
35. Giannelis EP, Krishinamoorti R, Manias E. Polymer-silicate nanocomposites: Model systems for confined polymers and polymer brushes. Adv. Polym. Sci. 138: 107-147 (1999)
36. LeBaron PC, Wang Z, Pinnavaia TJ. Polymer-layered silicate nanocomposites: An overview. Appl. Clay Sci. 15: 11-29 (1999)
37. Ogawa M, Kuroda K. Preparation of inorganic-organic nanocomposites through intercalation of organoammonium ions into layered silicates. Bull. Chem. Soc. Jpn. 70: 2593-2618 (1997)
38. Lagaly G. Introduction: From clay mineral-polymer interactions to clay mineral-polymer nanocomposites. Appl. Clay Sci. 15: 1-9 (1999)
39. Uyama H, Kuwabara M, Tsujimoto T, Nakano M, Usuki A, Kobayashi S. Green nanocompositefrom renewable resources: Plant oil-clay hybrid materials. Chem. Mater. 15: 2492-2494 (2003)
40. Kumar S, Jog JP, Natarajan U. Preparation and characterization of poly(methylmethacrylate)-clay nanocomposites via melt intercalation: The effect of organoclay on the structure and thermal properties. J. Appl. Polym. Sci. 89: 1186-1194 (2003)
41. Su SP, Wilkie CA. Exfoliated poly(methylmethacrylate) and polystyrene nanocomposites occur when the clay cations containing vinyl monomer. J. Polym. Sci. A1 41: 1124-1135 (2003)
42. Shen Z, Simon GP, Cheng YB. Comparison of solution intercalation and melt intercalation of polymer-clay nanocomposites. Polymer 43: 4251-4260 (2002)
43. Artzi N, Nir Y, Narkis M, Siegmann A. Melt blending of ethylene vinyl alcohol copolymer/clay nanocomposites: Effect of the clay type and processing conditions. J. Polym. Sci. Pol. Phys. 40: 1741-1753 (2002)
44. Wan C, Qiao X, Zhang Y, Zhang Y. Effect of different clay treatment on morphology and mechanical properties of PVC-clay nanocomposites. Polym. Test. 22: 453-461 (2003)
45. Suh DJ, Lim YT, Park OO. The property and formation mechanism of unsaturated polyester-layered silicate nanocomposite depending on the fabrication methods. Polymer 41: 8557-8563 (2000)
46. Choi HJ, Kim SG, Hyun YH, Jhon MS. Preparation and rheological characteristics of solvent-cast poly(ethylene oxide)/montmorillonite nanocomoposites. Macromol. Rapid Comm. 22: 320-325 (2001)
47. Ogata N, Kawakage S, Ogihara T. Poly(vinyl alcohol)-clay and poly(ethylene oxide)-clay blend prepared using water as solvent. J. Appl. Polym. Sci. 66: 573-581 (1997)
48. Aranda P, Ruiz-Hitzky E. Poly(ethylene oxide)-silicate intercalation materials. Chem. Mater. 4: 1395-1403 (1992)
49. Strawhecker KE, Manias E. Structure and properties of poly(vinyl alcohol)/Na^+ montmorillonite nanocomposites. Chem. Mater. 12: 2943-2949 (2000)
50. Greenland DJ. Adsorption of poly(vinyl alcohols) by montmorillonite. J. Coll. Sci. 18: 647-664 (1963)
51. Jimenez G, Ogata N, Kawai H, Ogihara T. Structure and thermal/mechanical properties of poly(ε-caprolactone)-clay blend. J. Appl. Polym. Sci. 64: 2211-2220 (1997)
52. Ogata N, Jimenez G, Kawai H, Ogihara T. Structure and thermal/mechanical properties of poly(*l*-lactide)-clay blend. J. Polym. Sci. Pol. Phys. 35: 389-396 (1997)
53. Jeon HG, Jung HT, Lee SW, Hudson SD. Morphology of polymer silicate nanocomposites: High density polyethylene and a nitrile. Polym. Bull. 41: 107-113 (1998)
54. Usuki A, Kojima Y, Kawasumi M, Okada A, Fukushima Y, Kurauchi T, Kamigaito O. Synthesis of nylon 6-clay hybrid. J. Mater. Res. 8: 1179-1184 (1993)
55. Li XC, Ha CS. Nanostructure of EVA/organoclay nanocomposites: Effects of kinds of organoclay and grafting of maleic anhydride onto EVA. J. Appl. Polym. Sci. 87: 1901-1909 (2003)
56. Huang M, Yu J. Structure and properties of thermoplastic corn starch/montmorillonite biodegradable composites. J. Appl. Polym. Sci. 99: 170-176 (2006)
57. Yano K, Usuki A, Okad A. Synthesis and properties of polyimide-clay hybrid films. J. Polym. Sci. A1 35: 2289-2294 (1997)
58. Yano K, Usuki A, Okad A, Kurauchi T, Kamigaito O. Synthesis and properties of polyimide-clay hybrid. J. Polym. Sci. A1 31: 2493-2498 (1993)
59. Cussler EL, Highes SE, Ward WJ, Aris R. Barrier membranes. J. Membrane Sci. 38: 161-174 (1998)
60. Polymer Nanocomposite Technology Brief. pp. 1-2. available from: http://ip.research.sc.edu/PDF/Polymer%20Nanocomposite%20Technology%20Brief%20v1.pdf. Accessed Dec. 27, 2006.
61. Zeng QH, Yu AB, Lu GQM, Paul DR. Clay-based polymer nanocomposites: Research and commercial development. J. Nanosci. Nanotechno. 5: 1574-1592 (2005)
62. Sinha Ray S, Yamad K, Okamoto M, Ueda K. Biodegradable polylactide/montmorillonite nanocomposites. J. Nanosci. Nanotechno. 3: 503-510 (2003)
63. Sinha Ray S, Yamada K, Okamoto M, Ueda K. Polylactide-layered silicate nanocomposite: A novel biodegradable material. Nano Lett. 2: 1093-1096 (2002)
64. Sinha Ray S, Yamada K, Okamoto M, Ueda K. New polylactide-layered silicate nanocomposites. 2. Concurrent improvements of material properties, biodegradability, and melt rheology. Polymer 44: 857-866 (2003)
65. Lee SR, Park HM, Lim H, Kang T, Li X, Cho WJ, Ha CS. Microstructure, tensile properties, and biodegradability of aliphatic polyester/clay nanocomposites. Polymer 43: 2495-2500 (2002)
66. Rhim JW, Hong SI, Park HM, Ng PKW. Preparation and characterization of chitosan-based nanocomposite films with antimicrobial activity. J. Agr. Food Chem. 54: 5814-5822 (2006)
67. Park JH, Jana SC. Mechanism and exfoliation of nanoclay particles in epoxy-clay nanocomposites. Macromolecules 36: 2758-2768 (2003)
68. Chen C, Curliss D. Processing and morphological development of montmorillonite epoxy nanocomposites. Nanotechnology 14: 643-648 (2003)
69. Messersmith PB, Gianellis EP. Synthesis and characterization of layered silicate-epoxy nanocomposites. Chem. Mater. 6: 1719-1725 (1994)
70. Okamoto M, Morita S, Kim YH, Kotaka T, Tateyama H. Dispersed structure change of smectic clay/poly(methyl methacrylate) nanocomposites by copolymerization with polar comonomers. Polymer 42: 1201-1206 (2001)
71. Okamoto M, Morita S, Taguchi H, Kim YH, Kotaka T, Tateyama H. Synthesis and structure of smectic clay/poly(methyl methacrylate) and clay/polystyrene nanocomposites via *in situ* intercalative polymerization. Polymer 41: 3887-3890 (2000)
72. Lu H, Hu Y, Yang L, Wang Z, Chen Z, Fan W. Preparation and thermal characteristics of silane-grafted polyethylene/montmorillonite nanocomposites. J. Mater. Sci. 40: 43-46 (2005)
73. Alexandre M, Dubois P, Sun T, Graces JM, Jerome R. Polyethylene-layered silicate nanocomposites prepared by the polymerization-filling technique: Synthesis and mechanical properties. Polymer 43: 2123-2132 (2002)
74. Wang KH, Choi MH, Koo CM, Choi YS, Chung IJ. Synthesis and characterization of maleated polyethylene/clay nanocomposites.

Polymer 42: 9819-9826 (2001)
75. Maiti P, Nam PH, Okamoto M, Hasegawa N, Usuki A. Influence of crystallization on intercalation, morphology, and mechanical properties of polypropylene/clay nanocomposites. Macromolecules 35: 2042-2049 (2002)
76. Kawasumi M, Hasegawa N, Kato M, Usuki A, Okada A. Preparation and mechanical properties of polypropylene-clay hybrids. Macromolecules 30: 6333-6338 (1997)
77. Cho JW, Paul DR. Nylon 6 nanocomposites by melt compounding. Polymer 42: 1083-1094 (2001)
78. Kojima Y, Usuki A, Kawasumi M, Okada A, Fukushima Y, Kurauchi T, Kamigaito O. Mechanical properties of nylon 6-clay hybrid. J. Mater. Res. 8: 1185-1189 (1993)
79. Cheng D, Xia H, Chen HSO. Synthesis and characterization of surface-functionalized conducting polyaniline-chitosan nanocomposite. J. Nanosci. Nanotechno. 5: 466-473 (2005)
80. Yeh JM, Chen YC, Ma CY, Lee KR, Wei Y, Li SI. Enhancement of corrosion protection effect of poly(*o*-ethoxyaniline) via the formation of poly(*o*-ethoxyaniline)-clay nanocomposite materials. Polymer 43: 2729-2736 (2002)
81. Sinha Ray S, Okamoto M. Biodegradable polylactide and its nanocomposites: Opening a new dimension for plastics and composites. Macromol. Rapid Comm. 24: 815-840 (2003)
82. Maiti P, Kazunobu K, Okamoto M, Ueda K, Okamoto K. New polylactide/layered silicate nanocomposites: Role of organoclays. Chem Mater. 14: 4654-4661 (2002)
83. Messersmith PB, Gianelis EP. Synthesis and barrier properties of poly(ε-caprolactone)-layered silicate nanocomposites. J. Polym. Sci. A1 33: 1047-1057 (1995)
84. Messersmith PB, Gianelis EP. Polymer-layered silicate nanocomposites: *In situ* intercalative polymerrization of ε-caprolactone in layered silicates. Chem. Mater. 5: 1064-1066 (1993)
85. McGlashan SA, Halley PJ. Preparation and characterization of biodegrdable starch-based nanocomposite materials. Polym. Int. 52: 1767-1773 (2003)
86. Tomka I. Thermoplastic starch. Adv. Exp. Med. Biol. 302: 627-637 (1991)
87. De Carvalho AJF, Curvelo AAS, Agnelli JAM. A first insight on composites of thermoplastic starch and kaolin. Carbohyd. Polym. 45: 189-194 (2001)
88. Park HM, Li X, Jin CZ, Park CY, Cho WJ, Ha CS. Preparation and properties of biodegradable thermoplastic starch/clay hybrids. Macromol. Mater. Eng. 287: 553-558 (2002)
89. Park HM, Lee WK, Park CY, Cho WJ, Ha CS. Environmentally friendly polymer hybrids. Part I. Mechanical, thermal, and barrier properties of thermoplastic starch/clay nanocomposites. J. Mater. Sci. 38: 909-915 (2003)
90. Wilhelm HM, Sierakowski MR, Souza GP, Wypych F. Starch films reinforced with mineral clay. Carbohyd. Polym. 52: 101-110 (2003)
91. Xu Y, Zhou J, Hanna MA. Melt-intercalation starch acetate nanocomposite forms as affected by type of organoclay. Cereal Chem. 82: 105-110 (2005)
92. Kester JJ, Fennema OR. Edible films and coatings: A review. Food Technol.-Chicago 40: 47-59 (1986)
93. Park HM, Misra M, Drzal LT, Mohanty AK. "Green" nanocomposites from cellulose acetate bioplastic and clay: Effect of eco-friendly triethyl citrate plasticizer. Biomacromolecules 5: 2281-2288 (2004)
94. Park HM, Liang X, Mohanty AK, Misra M, Drzal LT. Effect of compatibilizer on nanostructure of the biodegradable cellulose acetate/organoclay nanocomposites. Macromolecules 37: 9076-9082 (2004)
95. Cho MS, Choi SH, Nam JD, Lee Y. Preparation and mechanical properties of nanocomposite of cellulose diacetate/mentmorillonite. Polymer (Korea) 28: 551-555 (2004)
96. Ruan D, Zhang L, Zhang Z, Xia X. Structure and properties of regenerated cellulose/tourmaline nanocrystal composite films. J. Polym. Sci. Pol. Phys. 42: 367-373 (2003)
97. Zhang L, Ruan D, Gao S. Dissolution and regeneration of cellulose in NaOH/thiourea aqueous solution. J. Polym. Sci.: Part B: Polym. Phys. 40: 1521-1529 (2002)
98. Dufresne A, Vignon MR. Improvement of starch film performances using cellulose microfibrols. Macromolecules 31: 2693-2696 (1998)
99. Berglund L. Cellulose-based nanocomposites. pp. 808-832. In: Natural Fibers, Biopolymers, and Biocomposites. Mohanty AK, Misra M, Drzal LT (eds). CRC Press, Boca Raton, FL, USA (2005)
100. Lu Y, Weng L, Zhang L. Morphology and properties of soy protein isolate thermoplastics reinforced with chitin whiskers. Biomacromolecules 5: 1046-1051 (2004)
101. Nair KG, Dufresene A. Crab shell chitin whisker reinforced natural rubber nanocomposites. 1. Processing and swelling behavior. Biomacromolecules 4: 657-665 (2003)
102. Nair KG, Dufresene A. Crab shell chitin whisker reinforced natural rubber nanocomposites. 2. Mechanical behavior. Biomacromolecules 4: 666-674 (2003)
103. Eichhorn SJ, Baillie CA, Zafeiropoulos N, Mwaikambo LY, Ansell MP, Dufresne A, Entwistle KM, Herrera-Franco PJ, Escamilla GC, Groom L, Hughs M, Hill C, Rials TG, Wild PM. Current international research into cellulose fibers and composites. J. Mater. Sci. 36: 2107-2131 (2001)
104. Curvelo AAS, Carvalho AJF, Agnelli JAM. Thermoplastic starch-cellulose composites: Preliminary results. Carbohyd. Polym. 45: 183-188 (2001)
105. Anglès MN, Dufresne A. Plasticized starch/Tunicin whiskers nanocomposites. 1. Structural analysis. Macromolecules 33: 8344-8354 (2000)
106. Anglès MN, Dufresne A. Plasticized starch/Tunicin whiskers nanocomposites. 2. Mechanical behavior. Macromolecules 34: 2921-2931 (2001)
107. Dufresne A, Dupeyre D, Vignon MR. Cellulose microfibrils from potato tuber cells: Processing and characterization of starch-cellulose microfibril composites. J. Appl. Polym. Sci. 76: 2080-2092 (2000)
108. Baumberger S, Lapierre C, Monties B, Della Valle G. Use of kraft lignin as filler for starch films. Polym. Degrad. Stabil. 59: 273-277 (1998)
109. Dufresne A. High performance nanocomposite materials from thermoplastic matrix and polysaccharide fillers. Recent Res. Devel. Macromol. Res. 3: 455-474 (1998)
110. Dufresne A, Cavaillé JY, Helbert W. Thermoplastic nanocomposites filled with wheat straw cellulose whiskers. Part II: Effect of processing and modeling. Polym. Composite 18: 198-210 (1997)
111. Helbert W, Cavaillé JY, Dufresne A. Thermoplastic nanocomposites filled with wheat straw cellulose whiskers. Part I: Processing and mechanical behavior. Polym. Composite 17: 604-611 (1996)
112. Dufresne A, Cavaillé JY, Helbert W. New nanocomposite materials: Microcrystalline starch reinforced thermoplastic. Macromolecules 29: 7624-7626 (1996).
113. Lin KF, Hsu CY, Huang TS, Chiu WYM, Lee YH, Young TH. A novel method to prepare chitosan/montmorillonite nanocomposites. J. Appl. Polym. Sci. 98: 2042-2047 (2005)
114. Xu Y, Ren X, Hanna MA. Chitosan/clay nanocomposite film preparation and characterization. J. Appl. Polym. Sci. 99: 1684-1691 (2006)
115. Wang SF, Shen L, Tong YJ, Chen L, Phang IY, Lim PQ, Liu TX. Biopolymer chitosan/montmorillonite nanocomopsites: Preparation and characterization. Polym. Degrad. Stabil. 90: 123-131 (2005)
116. Rhim JW. Effect of clay concentration on mechanical and water barrier properties of chitosan-based nanocomposite films. Food Sci. Biotechnol. 15: 925-930 (2006)
117. Darder M, Colilla M, Ruiz-Hitzky E. Biopolymer-clay nanocomposites based on chitosan intercalated in montmorillonite. Chem. Mater. 15: 3774-3780 (2003)
118. Otaigbe JU, Adams DO. Bioabsorbable soy protein plastic composites: Effect of polyphosphate fillers on water absorption and mechanical properties. J. Environ. Polym. Degr. 5: 199-208 (1997)
119. Rhim JW, Lee JH, Kwak HS. Mechanical and barrier properties of soy protein and clay mineral composite films. Food Sci. Biotechnol. 14: 112-116 (2005)
120. Dean K, Yu L. Biodegrdable protein-nanocomposites. pp. 289-309. In: Biodegradable Polymers for Industrial Application. Smith R

(ed). CRC Press, Boca Raton, FL, USA (2005)
121. Zheng JP, Li P, Ma YL, Yao KD. Gelatin/montmorillonite hybrid nanocomposite. I. Preparation and properties. J. Appl. Polym. Sci. 86: 1189-1194 (2002)
122. Ozdemir M, Floros JD. Active food packaging technology. Crit. Rev. Food Sci. 44: 185-193 (2004)
123. Vermeiren L, Devlieghere F, van Beest M, de Kruijf N, Debevere J. Developments in active packaging of foods. Trends Food Sci. Tech. 10: 77-86 (1999)
124. Cha DS, Chinnan MS. Biopolymer-based antimicrobial packaging: A review. Crit. Rev. Food Sci. 44: 223-237 (2004)
125. Cagri A, Ustunol Z, Ryser ET. Antimicrobial edible films and coatings. J. Food Protect. 67: 833-848 (2004)
126. Labuza TP, Breene WM. Applications of active packaging for improvement of shel-life and nutritional quality of fresh and extended shelf-life foods. J. Food Process Pres. 13: 1-69 (1989)
127. Han JH, Floros JD. Casting antimicrobial packaging films and measuring their physical properties and antimicrobial activity. J. Plast Film Sheet 13: 287-289 (1997)
128. Weng YM, Chen MJ. Sorbic anhydride and antimicotic additive in polyethylene food packaging films. Food Sci. Technol. 30: 485-487 (1997)
129. Ming X, Weber GH, Ayres JW, Sandine WE. Bacteriocin applied to food packaging materials to inhibit *Listeria monocytogenes* on meats. J. Food Sci. 62: 423-415 (1997)
130. Padgett T, Han IY, Dawson PL. Incorporation of food-grade antimicrobial compounds into biodegradable packaging films. J. Food Protect. 61: 1130-1335 (1998)
131. Ishitani T. Active packaging for food quality preservation in Japan. pp. 177-188. In: Foods and Packaging Materials-Chemical Interactions. Ackerman P, Jagerstad M, Oglsson M (eds). Royal Society of Chemistry, Cambridge, UK (1995)
132. Halek W, Garg A. Fungal inhibition by a fungicide coupled to an ionomeric film. J. Food Safety 9: 215-222 (1989)
133. Weng YM, Hochkiss JH. Inhibition of surface molds on cheese by polyethylene film containing the antimycotic imazalil. J. Food Protect. 55: 367-369 (1992)
134. Del Nobile MA, Cannaris M, Altieri C, Sinigaglia M, Favia P, Iacoviello G, D'Agostino R. Effect of Ag-containing nano-composite active packaging system on survival of *Alicyclobacillus acidoterrestris*. J. Food Sci. 69: E379-E383 (2004)
135. Siragusa GA, Dickson JS. Inhibition of *Listeria monocytogenes* on beef tissue by application of organic acids immobilized in a calcium alginate gel. J. Food Sci. 57: 293-296 (1992)
136. Torres JA, Motoki M, Karel M. Microbial stabilization of intermediate moisture food surfaces. I. Control of surface preservative concentration. J. Food Process. Pres. 9: 75-92 (1985)
137. Ouattara B, Simard RE, Piette G, Begin A, Holley RA. Inhibition of surface spoilage bacteria in processed meats by application of antimicrobial films prepared with chitosan. Int. J. Food Microbiol. 62: 139-148 (2000)
138. Coma V, Martial-Gros A, Garreau S, Copinet A, Salin F, Deschamps A. Edible antimicrobial films based on chitosan matrix. J. Food Sci. 67: 1162-1169 (2002)
139. Weng YM, Hochkiss JH. Anhydrides as antimycotic agents added to polyethylene films for food packaging. Packag. Technol. Sci. 6: 123-128 (1993)
140. Park SI, Daeschel MA, Zhao Y. Functional properties of antimicrobial lysozyme-chitosan composite films. J. Food Sci. 69: 215-221 (2004)
141. Coma V, Deschamps A, Martial-Gros A. Bioactive packaging materials from edible chitosan polymers - Antimicrobial activity assessment on dairy-related contaminants. J. Food Sci. 68: 2788-2792 (2003)
142. Gällstedt M, Hedenqvist MS. Oxygen and water barrier properties of coated whey protein and chitosan films. J. Polym. Environ. 10: 1-4 (2002)
143. Park SY, Marsh KS, Rhim JW. Characteristics of different molecular weight chitosan films affected by the type of organic solvents. J. Food Sci. 67: 194-197 (2002)
144. Rhim JW, Weller CL, Ham KS. Characteristics of chitosan films as affected by the type of solvent acid. Food Sci. Biotechnol. 7: 263-268 (1998)
145. Rabea EI, Badawy MET, Stevens CV, Smagghe G, Steurbaut W. Chitosan as antimicrobial agent: Application and mode of action. Biomacromolecules 4: 1457-1465 (2003)
146. Ikejima T, Inoue Y. Crystallization behavior and environmental biodegradability of the blend films of poly(3-hydroxybutyric acid) with chitin and chitosan. Carbohyd. Polym. 41: 351-356 (2000)
147. Olabarrieta I, Forsstrom D, Gedde UW, Hedenqvist MS. Transport properties of chitosan and whey blended with poly(ε-caprolactone) assessed by standard permeability measurements and microcalorimetry. Polymer 42: 4401-4406 (2001)
148. Senda T, He Y, Inoue Y. Biodegradable blends of poly(ε-caprolactone) with α-chitin and chitosan: specific interactions, thermal properties, and crystallization behavior. Polym. Int. 51: 33-39 (2001)
149. Suyatma NE, Copinet A, Tighzert L, Coma V. Mechanical and barrier properties of biodegradable films made from chitosan and poly(lactic acid) blends. J. Polym. Environ. 12: 1-6 (2004)
150. Liao Y, Wang Q, Xia H. Preparation of poly(butyl methacrylate)/γ-Al_2O_3 nanocomposites via ultrasonic irradiation. Polym. Int. 50: 207-212 (2002)
151. Hugo WB, Russel AD. Types of antimicrobial agents. pp. 7-68. In: Principles and Practice of Disinfection, Preservation, and Sterilization. Russel AD, Hugo WB, Ayliffe GAJ (eds). Blackwell Scientific Publications, Oxford, UK (1992)
152. Kim CH, Choi JW, Chun HJ, Choi SK. Synthesis of chitosan derivatives with quarternary ammonium salt and their antibacterial activity. Polym. Bull. 38: 387-393 (1997)
153. Gottenbos B, Van der Mei HC, Klatter F, Nieuwenhuis P, Busscher HJ. *In vitro* and *in vivo* antimicrobial activity of covalently coupled quarternary ammonium silane coatings on silicone rubber. Biomaterials 23: 1417-1423 (2002)
154. Kim JY, Lee JK, Lee TS, Park WH. Synthesis of chitooligosacharide derivative with quarternary ammonium group and its antimicrobial activity against *Streptococcus mutans*. Int. J. Biol. Macromol. 32: 23-27 (2003)
155. Wang X, Du Y, Yang J, Wang X, Shi X, Hu Y. Preparation, characterization, and antimicrobial activity of chitosan/layered silicate nanocomposites. Polymer 47: 6738-6744 (2006)